THE COMPARISON STUDY ON ULTRAVIOLET-A-INDUCED PHOTOAGING VERSUS AGING IN HUMAN DERMAL FIBROBLASTS

By

Weiqi Jiao

A thesis submitted to Johns Hopkins University in conformity with the requirements for the degree of Master of Science

Baltimore, Maryland
May 2021

ABSTRACT

Melanoma is an exceptionally aggressive and therapy-resistant cancer with an expanding incidence rate over the past few decades. Metastatic and recurrent melanoma responds poorly to therapy and has a high rate of mortality, despite prominent therapeutic progress. Overexposure to either natural or artificial ultraviolet radiation (UVR) causes a range of skin disorders including sunburn, premature aging, immunosuppression, and inflammatory reactions, and is a major risk factor for melanoma. UVA is particularly detrimental as it not only is the primary component of UVR reaching the earth surface and indoor tanning beds but also penetrates deeply into the dermis, reacting with the resident cells including fibroblasts and remodeling the extracellular matrix (ECM). The consequence of these alterations is photoaging and cancer. Previously, our lab has demonstrated that ECM remodeling is a key feature of chronological aging of human skin fibroblasts, which in turn can drive the aggressive nature of human melanoma. Therefore, we hypothesize that overexposure to UVA will induce changes in ECM-related gene expression in young fibroblasts that drive them towards an aged phenotype.

As hypothesized, this study reports that a sublethal dose of UVA irradiation induces a change from flattened to round shape in young fibroblasts collected from healthy people, which is a characteristic phenomenon in photoaged skin. Photoaging leads to distinct changes in cell shape, which loses intercellular contacts. Aligned

with this, the expression of β-catenin which is responsible for cell adhesion and functional in the Wnt signaling pathway is also reduced in fibroblasts. Conversely, the expression of MMP-1 which is responsible for denaturing ECM, is significantly increased in both the lysate and culture media of fibroblasts. In addition, more DNA damage occurs in irradiated fibroblasts than in aged or unirradiated cells. Our observations and analysis verify the photoaging effect of UVA irradiation in human dermal fibroblasts. Similar changes in the ECM-related protein expression observed in aged fibroblasts also implicate that UVA could drive them towards an aged, tumor-promoting phenotype. This may also emphasize and reveal the importance of effective preventions against melanoma, promoting factors and potential targets that can be targeted to overcome the disease.

Keywords*: Melanoma; Photoaging; UVA irradiation; Human dermal fibroblasts*

Advisor: Ashani T. Weeraratna, Ph.D.
Bloomberg Distinguished Professor of Cancer Biology
E.V. McCollum Chair of Biochemistry and Molecular Biology
Johns Hopkins Bloomberg School of Public Health.
And, Co-Program Leader, Cancer Invasion and Metastasis,
Sidney Kimmel Cancer Center, Hopkins School of Medicine

Thesis Advisor: Vito W. Rebecca, Ph.D.
Assistant Professor, Biochemistry and Molecular Biology
Johns Hopkins Bloomberg School of Public Health

TABLE OF CONTENTS

LIST OF FIGURES

1. INTRODUCTION

1.1 Public Health Burden of Melanoma

Skin cancer has been characterized as a major public health problem because of the persistent increase of incidence rate resulting in significant burden in the United States over the years (Watson et al., 2016). Cutaneous malignant melanoma, hereafter specified as melanoma, is a cancer of the skin generated from highly mutated epidermal melanocytes (Kaur et al., 2019), of which the incidence and mortality are systematically tracked all over the country (Watson et al., 2016). While a great deal of progress has been made in therapeutic advancements such as immune checkpoint inhibitors and targeted BRAF or MEK inhibition (Zhou et al., 2015), the melanoma incidence rate is still on the rise. The biggest challenge that remains is recurrent melanoma that shows poor response rates and is accompanied by severe adverse events highlighting the unmet needs for developing more effective methods to conquer melanoma (Zhou et al., 2015). Once the tumor has metastasized to distant locations, the 5-year survival rate of malignant melanoma is only 15-20% (Siegel et al., 2016). Due to the high metastatic potential and resistance to therapies, melanomas for nearly half of all skin cancer deaths despite only representing 10% of skin cancers (Pfeifer and Besaratinia, 2012). In order to reduce mortality when there is no developed treatment capable of prolonging patient survival with metastasis, an effective prevention strategy is needed for people at risk.

1.2 An Overview of Melanoma

Melanoma arises from the malignant transformation of pigment-producing of melanocytes that normally stay in the basal layer of the epidermis (Chin, 2003). The series of transitions outlined in Figure 1 show its development (Postovit et al., 2006). The subset of initial aberrant proliferating melanocytes begins to spread directly or through forming dysplastic naevi, this process is called radial growth phase (RGP) and is associated with a good prognosis(Postovit et al., 2006). When a transition to the next vertical growth phase (VGP) occurs, cells acquire the metastatic potential as they have broken away from the bulk melanoma and penetrated through the basement membrane(Postovit et al., 2006). Melanoma cells then can progress to metastasize, characterized by extensive vascularization and invasion. Each step along the developmental line requires spontaneous mutations in specific genes and the whole sequence of events may or may not occur during the lifetime of an individual (Meyle and Guldberg, 2009).

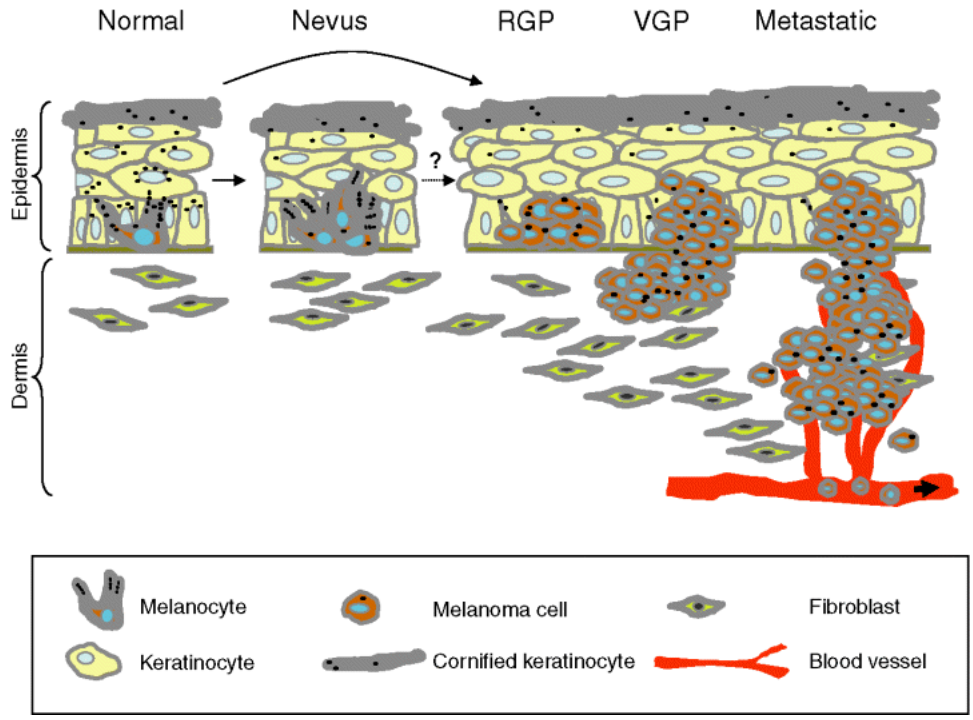

Figure 1. The development of malignant melanoma.

The progression of a melanocyte to malignant melanoma is represented. The development of naevi is a relatively frequent event but the transition of naevi to more malignant disease is relatively rare. Besides, the malignant disease may arise from melanocytes that do pass through the naevus stage(Gaggioli and Sahai, 2007).

As is the case with most cancer types, melanoma pathogenesis is driven by both genetic and environmental risk factors, influenced by skin pigmentation, sun exposure history, and geographical location(Chin, 2003). The genetic basis is complex with both inherited and acquired components (Meyle and Guldberg, 2009). With technological advances such as genome sequencing, new platforms to investigate single nucleotide polymorphism, and methylation patterns, the field of melanoma genetics is moving at a great pace and providing new insights into the potential biomarkers and therapeutic targets for this tumor (Ribero et al., 2016). Genome-wide association studies have revealed many rare and highly penetrant genes such as *CDKN2A*, *CDK4*, and lowly penetrant genes such as *MC1R*, *ASIP*, and *TYP*. (Marzuka-Alcalá et al., 2014). This is of importance in discovering pathways related to pigmentation, melanocyte transition, Naevus counts, and cell senescence(Ribero et al., 2016). For example, oncogenic BRAF mutations, which has been demonstrated in a large proportion of melanomas for activating the mitogen-activated protein kinase (MAPK) signaling pathway and up-regulating cell proliferation and invasive ability(Spathis et al., 2019), was found to significantly higher in *MC1R*-deficient individuals (Dhomen and Marais, 2007).

Cutaneous melanoma is caused by the interaction of variable environmental exposure, genetic susceptibility, and other host factors(Anne, 2018). Exposure to ultraviolet radiation (UVR) is another major etiological factor that is influenced by

many host factors such as tanning ability, skin color, and the number of naevi. Both UVR-induced mutations in melanocytes and changes in the immune microenvironment are known to play a role in the development of cutaneous melanoma(Emri et al., 2018). Primary melanomas are characterized by mutations in *BRAF*, *NRAS*, and *TERT*, but about 80% of melanomas carry UVR signature mutations (C–T or CC–TT)(Akbani et al., 2015). Another study in an *HGF*-transgenic/*CDK4 R24C*-mutated mouse melanoma model found that UV exposure resulted in neutrophil cell infiltration and activation in the tumor, which was also observed to promote angiotropic tumor progression and metastasis(Bald et al., 2014). Although a great amount of data has provided an overview of how major UVR affects skin cancer, the pathogenetic role of signaling pathways driving melanoma progression is not fully understood.

1.3 Risks of Natural and Artificial Sunlight Exposure

There is a strong and sufficient body of experimental evidence that UVR causes melanoma, as well as epidemiological observations of elevated incidence rates in sun-sensitive and fair-skinned populations compared to their darker-skinned counterparts(El Ghissassi et al., 2009)(Erdmann et al., 2013). As a complete carcinogen, exposure to UVR is mainly through radiation from the sun. Solar UVR can interact with many kinds of molecules in the human skin, which may have both positive and negative biological effects depending on the UV sources, exposure, and wavelength(Pérez-Sánchez et al., 2018). The positive effects include promoting vitamin D synthesis and treating some skin disorders such as psoriasis and potentially for systemic autoimmune diseases such as multiple sclerosis(Lucas et al.,

2019). Most people can synthesize sufficient vitamin D from daily short-periods of sun exposure on their forearms, hands, or lower legs uncovered(Pérez-Sánchez et al., 2018). However, inappropriately high exposure to UV radiation for the individual's skin type causes sunburn which ranges from a short-lived mild reddening of the skin to painful blisters that last several days. Other inflammatory reactions of the skin (photodermatoses) occur in people who are abnormally sensitive to UV radiation(Lucas et al., 2019). According to a U.S. National Health Interview Survey in 2010, sunburn is common among U.S. adults, the highest prevalence was observed among adults aged 18-29(52.0%) and is also especially among those who are most susceptible to skin cancer (i.e., whites, those with skin that burns repeatedly, and those with a family history of melanoma)(Holman et al., 2014). The health risks of sun exposure can be mitigated through appropriate sun protection behaviors depending on an individual's susceptibility to UVR exposure(Shih et al., 2018). Recommendations are that when the UV index provided by weather forecasts and several apps for mobile phones is 3 or higher, protection should be used(Lucas et al., 2019). Protection involves a suite of options, such as staying out of the sun, wearing clothing, hats, and sunglasses, best used in combination. Sunscreen is typically the second line of defense and particularly useful for body surfaces that cannot be covered by clothing (e.g. face and hands). Despite it is the most frequently nominated protection strategy, health experts have voiced concerns about flawed application practices and protective clothing and shade are better options in current sun-protection hierarchies (Koch et al., 2017).

In addition, indoor tanning as the main source of non-natural sunlight is also responsible for the increase in melanoma incidence rates, especially along with young

women(Guy et al., 2017b). The World Health Organization (WHO) and the US Department of Health and Human Services have classified UV-emitting indoor tanning devices as carcinogenic to human beings(El Ghissassi et al., 2009). Importantly, a single tanning session increases a user's risk of cutaneous melanoma by 20%(Boniol et al., 2012), the risk is even higher among frequent tanners and those initiating indoor tanning before the age of 20(Boniol et al., 2012).

Despite public health efforts by the WHO, the number and use of indoor tanning devices have skyrocketed over years. In the late 1980s, only 1% of the American population had ever used the tanning bed(Trapani et al., 2020), while in 2015, nearly 7.8 million American adults still utilized indoor tanning devices(Guy et al., 2017a). This is an important industry with dozens of millions of clients and billions of dollars of annual business. But these devices are poorly regulated and vary greatly concerning UV composition and strength which could be up to ten times more powerful than natural sunlight(Nilsen et al., 2011), making it a continued public health problem. The US Surgeon General has emphasized the importance of reducing the risks from indoor tanning(Watson et al., 2014).

1.4 The Skin

Skin pigmentation is among the most important determinants of UV sensitivity and skin cancer risk(D'Orazio et al., 2013). Human skin is composed of three main layers with different underlying structures: (a) the epidermis primarily consisting of keratinocytes and melanocytes, (b) the dermis containing abundant immune cells and fibroblasts, (c) the hypodermis serving as the energy storage area(Pérez-Sánchez et al., 2018). The epidermis is a self-renewing tissue of which the

biological and physical characteristics play a significant role in resisting environmental stressors like infectious pathogens, chemicals, and UV light(Slominski et al., 2012). In addition to forming an effective physical barrier, keratinocytes also function to block UV penetration into the skin through accumulating melanin pigments as they mature(D'Orazio et al., 2013). Epidermal melanin is the major factor determining the skin complexion and UV sensitivity that is found in two major forms: the dark highly UV-protective eumelanin pigment and the red/blonde UV-permeable pheomelanin. (Slominski et al., 2004). Thus, fair-skinned people that have little epidermal eumelanin are much more UV-sensitive and have a higher risk of skin cancer than darker-skinned people(Vincensi et al., 1998).

Underlying the epidermis, the dermis is also a layer that is mostly composed of complex extracellular matrix (ECM) proteins and collagen fibers largely secreted by dermal fibroblasts, actively participate in many physiological responses(Fuchs and Raghavan, 2002). ECM is a three-dimensional network of macromolecules that support the critical structural and biomechanical function of each organ (Mouw et al., 2014). The diversity of ECM components contributes to the extreme complexity of the tumor microenvironment, such as laminin, collagen, growth factors, nutrients, and varying concentrations of oxygen. Collectively, a normal ECM provides the necessary architecture that supplies signals to control cell phenomena(Postovit et al., 2006). The dysregulation of ECM will cause aberrant interactions and mechanical deficiency, and correspondingly increase the risk for pathogenesis and susceptibility of cancer colonization and metastasis(Marino and Weeraratna, 2020). For example, studies have elucidated the ability of the microenvironment to epigenetically transdifferentiate melanocytes toward an invasive melanoma phenotype(Seftor et al.,

2005). Other proteolysis research of ECM components has shown that matrix metalloproteinases (MMP) are upregulated in invasive melanoma and play a vital role in promoting the dissemination of melanoma(Hofmann et al., 2005)(Thakur and Bedogni, 2016)(Zaman et al., 2019).

1.5 Cutaneous Response to Ultraviolet Irradiation

UVR has numerous effects on skin physiology with both acute and long-term consequences (D'Orazio et al., 2013). Since UVC is almost completely blocked by the ozone layer, ultraviolet radiation reaching the earth's surface is composed primarily of UVA (90–95%) and UVB (5–10%). As shown in Figure 2, UV penetrates the skin in a wavelength-dependent manner(Pérez-Sánchez et al., 2018).

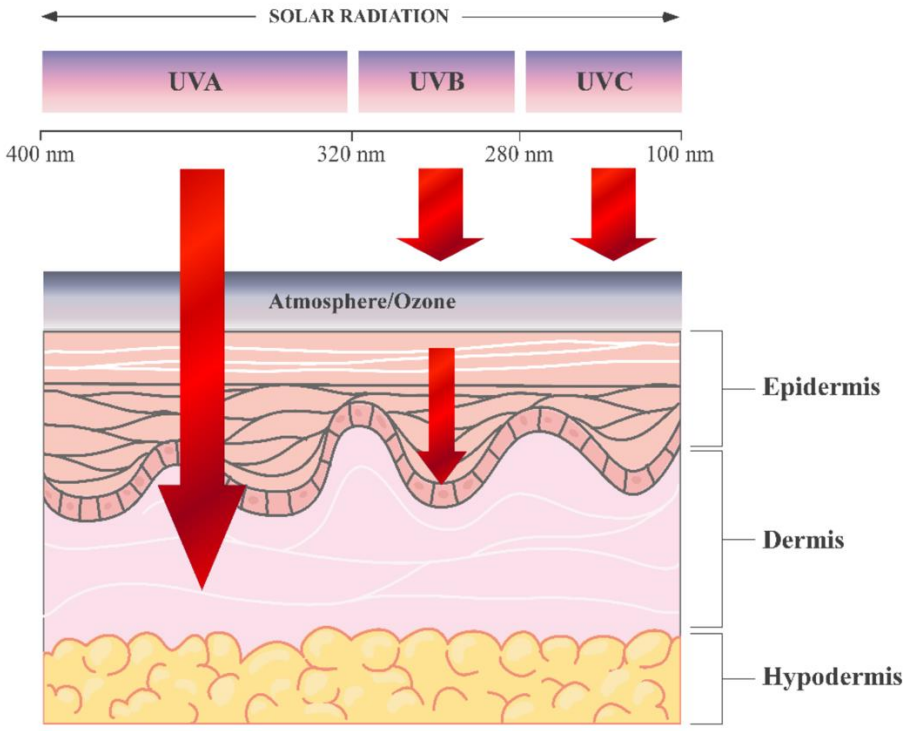

Figure 2. UV penetration into the layers of the skin.

UVA (longer wavelength) reaching the dermis and UVB is almost entirely absorbed by the epidermis(Pérez-Sánchez et al., 2018). The figure was created using Servier

Medical Art (

Both UVA and UVB can directly damage DNA molecules or induce the formation of pyrimidine dimers between adjacent pyrimidine bases, which result in mutations(Douki et al., 2017). Inflammation and “sunburn” are examples of the most obvious acute effects caused by UVB damage to keratinocytes, the response cascade of cytokines(Coelho et al., 2009). UVB is thus highly studied for resulting in immunosuppression via altering the function of antigen-presenting cells in the epidermis, the formation of cyclobutane pyrimidine dimers (CPDs) that may lead to DNA mutations and cancer(Naylor et al., 2011). Coupled with these epidermal changes, UVB stimulates the melanogenic system with melanin pigment production upregulated and accumulated in the skin, also known as adaptive melanization or tanning(Coelho et al., 2009). Although UVB is more arrhythmogenic than UVA radiation, it only represents a minority part of the irradiation and is almost entirely absorbed by the epidermis(D’Orazio et al., 2013).

Indoor tanning devices emit a low fraction of UVB rays (<5%) but unnaturally high levels of UVA(Boniol et al., 2012). UVA does not affect melanin content, yet stimulates skin pigmentation significantly presumably due to the oxidation of melanin, effect on the distribution of melanosomes, and perhaps the effects on cytoskeleton components(Jimbow and Fitzpatrick, 1975). UVA radiation is also detrimental as it penetrates deeply into the dermis causing damage to the cells, such as fibroblasts which are resident in the deeper layers of the skin(Holick, 2016). On the one hand, at cellular and molecular levels, chronic UVA exposure induces the formation of reactive oxygen species (ROS) which can reduce immune response, and

cause prolonged changes in dermal structure, gene expression, and ECM via indirect photosensitizing reactions(Battie et al., 2014). Nucleotides are highly susceptible to free radical injury and easily mispairing between bases after their oxidation, causing mutagenesis(Schulz et al., 2000). Such mutations have been found in tumors in the skin, suggesting that oxidative injury can be carcinogenic(Agar et al., 2004). On the other hand, UVA radiation increases MMPs expression in the dermis, which are responsible for degrading ECM proteins and affecting several processes in carcinogenesis such as tumor growth, angiogenesis, and metastasis(O'Grady et al., 2007). As the equilibrium in the accumulation and degradation of ECM is disturbed by UVA, subsequent alterations including irregular pigmentation, dryness, and wrinkling(Ganceviciene et al., 2012). The consequence of these alterations is premature photoaging and carcinogenesis of the skin(Bai et al., 2018). These alterations may contribute to the malignant progression of melanoma.

1.6 Photoaging of the skin

Skin aging is a complex biological process resulting from synergistic intrinsic and extrinsic mechanisms(Pérez-Sánchez et al., 2018). Extrinsic aging is caused by environmental factors such as photoaging being a major contributor. As mentioned above, photoaging and photodamage can be avoided and are caused by repetitive exposure of the skin to harmful UV light. Chronically sun-exposed skin has the characteristic feature of a coarse, wrinkled appearance that is the hallmark of photoaged skin(Kligman and Kligman, 1986). In addition to changes in epidermal thickness, like atrophy or hyperplasia, photoaging is also complicated by alterations in the dermal cells and matrix(Min et al., 2014), as shown in Figure 3. Collagen fibrils

are largely responsible for the strength and resilience of skin, through inhibition of procollagen synthesis and upregulation of MMPs expression, UVA irradiation causes its reduction in the photoaged skin(Fisher et al., 1997). Other quantitative alterations including damaged collagen fibrils, disorganized elastic fibers, and accumulation of aberrant elastic materials have also been seen in the dermal connective tissue(Quan et al., 2009).

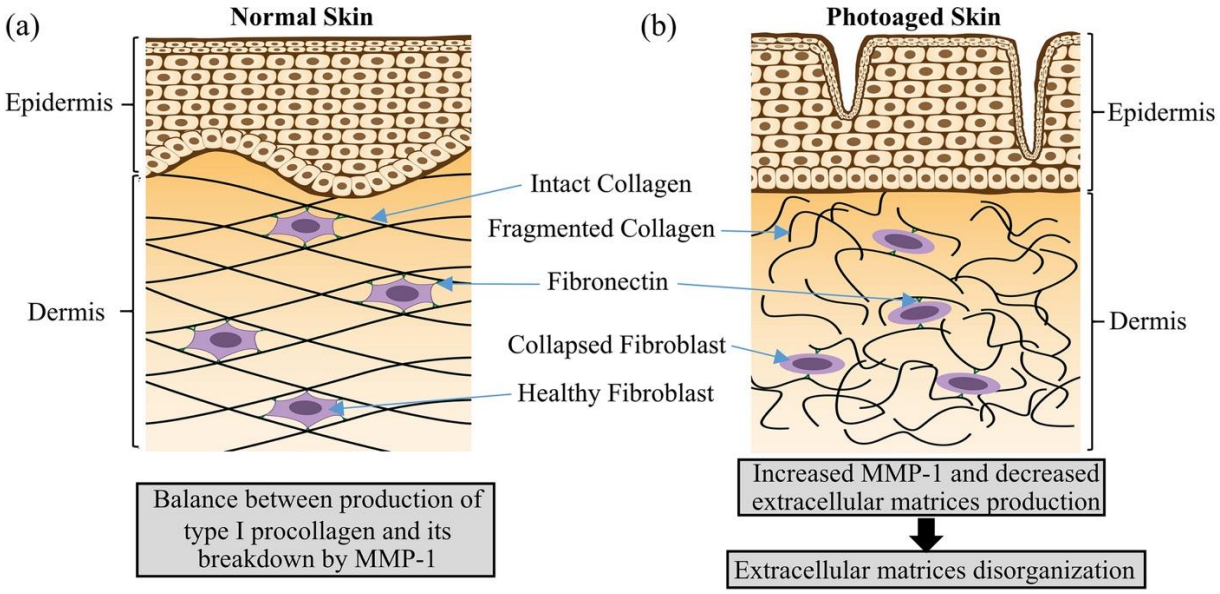

Figure 3. Illustration of (a) normal skin (b) photoaged skin

The photoaged skin results from repeated UVA exposure which causes the overproduction of MMP-1 by fibroblasts which in turn causes collagen degradation which produces an accumulation of fragmented collagen fibers. Decreased production of ECMs from the malfunction of fibroblasts found in skin dermal tissue also occurs from UVA exposure(Nakyai et al., 2017).

As the major cell component of the dermis, fibroblasts are the main source of ECM proteins such as type I, II, III collagens, elastin, fibronectin, and tenascin C (TNC), and are critical in the metabolism of ECM proteins by producing different types of enzymes including MMPs, lysyl oxidases, or lysyl hydroxylases (Liu et al., 2019). Its typically flattened or extensible shape in the dermis is a critical determinant

of their function, which changes corresponding to the extracellular environment (Varani et al., 2001). A previous study reported that UVA exposure induced morphological changes in human dermal fibroblasts (HDFs) from expanded to rounded which was caused by the destruction of actin filaments and responsible for the collagen reduction in photoaged skin(Yamaba et al., 2016). The dynamic properties of fibroblasts include altering cell-matrix interactions, cell-cell interactions, secreting proteins that control epithelial cell proliferation, and so on(Cuiffo and Karnoub, 2012). Unlike melanoma cells, fibroblasts are not the source of tumors but they are important in creating the pre-tumor microenvironment and orchestrating the complexity of TME(Liu et al., 2019). It appears that normal dermal fibroblasts have a repressive effect on the growth and progression of tumor cells at an early stage of tumor development(Cornil et al., 1991). However, under the stimulation of possible driving factors like platelet-derived growth factor (PDGF) and basic fibroblast growth factor (bFGF) that are secreted by tumor cells, normal fibroblasts can irreversibly enter into an active state, termed cancer-associated fibroblasts (CAFs), with the ability to remodel ECM and secrete growth factors, which altogether can encourage tumor growth(Zhou et al., 2015). As illustrated in Figure.4, abundant studies have revealed the mechanisms of action by which CAFs promote tumorigenesis through direct influence on malignant cells and recruiting other types of tumor cells, facilitate progression through remodeling ECM and angiogenesis (Gascard and Tlsty, 2016). Remarkably, the dysregulated cell-intrinsic signaling pathways underlying those diverse mechanisms can contribute to drug resistance and impair therapeutic responses(Castells et al., 2012). Therefore, further understanding of how fibroblasts become cancer-associated and then contribute to melanoma is

important for preventing the emergence of the tumor and developing more efficient treatments against it.

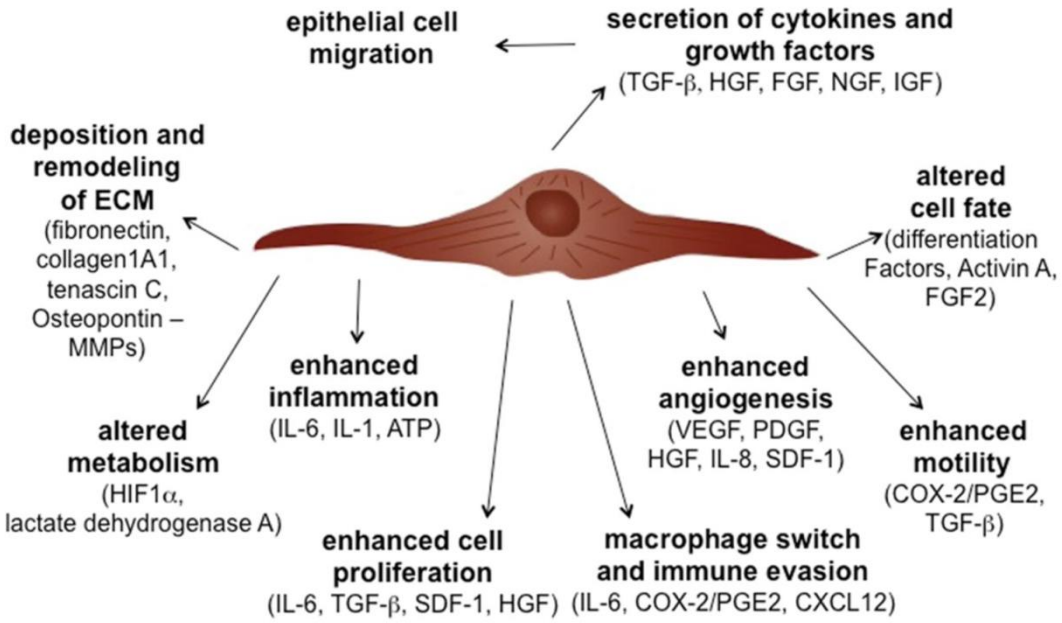

Figure 4. Multiple secreted factors and resultant phenotypes stimulated by Cancer-associated Fibroblasts (CAFs).

CAFs induce multiple phenotypes in neighboring tumor epithelial cells as well as other stromal cell types. Soluble factors secreted by CAFs have been involved in promoting each of these phenotypes(Gascard and Tlsty, 2016).

1.7 β-catenin Signaling Pathway in Melanoma-associated Fibroblasts

β-catenin is an evolutionarily conserved multifunctional protein involved in various cellular activities depending on its intracellular locations(Boivin et al., 2015), thus plays a crucial role in physiological homeostasis and a wide variety of human cancers(Liu et al., 2019). At the cell membrane, β-catenin binds to the intracellular domain of cadherin-cased adhesion junctions between adjacent cells, a process that is required for cell movements(Boivin et al., 2015). It is also an essential component in both Wnt signaling-mediated gene expression(Miller and Moon, 1996), In the

presence of WNT-ligands, cytosolic β-catenin is stabilized (non-phosphorylated), permitting it to serve as a transcriptional co-activator and interact with a wide range of transcription factors in the nucleus, activate several target genes including MMPs, growth factors, ECM proteins, pro-inflammatory mediators and enzymes(Baarsma et al., 2011) (Cheon et al., 2004).

In melanoma, Wnt/β-catenin signaling directly regulates the pigment cell lineages and the expression of a major determinant of both melanocyte development, microphthalmia transcription factor (MITF)(Dorsky et al., 2000). Studies have reported that the activation of Wnt/β-catenin signaling increases the proliferation of melanoma cells in cell culture and mouse models (Delmas et al., 2007)(Widlund et al., 2002). However, Wnt/β-catenin signaling is not oncogenic in any sense. Studies in patients have monitored that upregulation of Wnt/β-catenin signaling correlates with better prognosis as monitored in patients of primary or metastatic melanoma because it upregulates genes that are frequently lost in melanoma progression (Mælandsmo et al., 2003). Collectively, it is the disrupted homeostatic balance of Wnt/β-catenin signaling that leads to melanoma transformation.

As mentioned before, normal stromal fibroblasts could transform to reactive and tumor-promoting CAFs under the effects of multiple factors. It has been demonstrated that the activation of the canonical WNT/β-catenin signaling pathway is associated with fibroblast activation, fibrosis, and tissue repair(Baarsma et al., 2011). One previous study observed that *BRAF*-activated *PTEN*-deficient mouse melanoma growth was significantly suppressed when β-catenin in melanoma-associated fibroblasts was blocked after melanoma formation *in vivo*(Zhou et al., 2018). Interestingly, the same team also has discovered that the blocked β-catenin

expression could inhibit the normal biological function of stromal fibroblasts and B16 melanoma development was accelerated when the β-catenin expression was ablated in fibroblasts before tumor initiation(Zhou et al., 2016). Despite the abundant evidence demonstrating the significance of β-catenin activity in CAFs, the molecular mechanisms underlying the functional association between β-catenin and the ECM remodeling abilities of CAFs have not been fully described.

1.8 Natural Aging of the Skin

Different from photoaging, intrinsic or genetically programmed aging occurs with time. Endogenous aging is an inevitable phenomenon and an independent negative prognostic indicator of melanoma(Balch et al., 2014). The initial melanoma is diagnosed at a middle age of 63 and the highest percentage of melanoma-related deaths occur in patients aged 75–84(U.S. Surveillance, Epidemiology, and End Results Program (SEER)). Since melanoma is a very immunogenic tumor, insights into the natural history of melanoma in older patients are attributed to a reduction in naïve T cells, decreased T cell functionality due to loss of co-stimulatory molecules, T cell exhaustion, and reduction in pro-inflammatory cytokine secretion, compared with young patients(Hegde et al., 2009)(Weiss et al., 2016). Preceding studies have also observed an age-related increase of sFRP2 secreted by dermal fibroblasts, which activates a multi-step signaling cascade in melanoma cells. This age-related change ultimately augments both angiogenesis and metastasis of melanoma cells, also rendered them more resistant to targeted therapy (vemurafenib)(Kaur et al., 2016). Instead of inducing changes in tumor molecular pathways and host immune response, aging is associated with changed architectural properties of skin such as

decreased collagen density and ECM remodeling, which significantly affects the metastatic properties of tumor cells and in turn can drive the aggressive nature of human melanoma(Levental et al., 2009). The previous study has found that factors secreted by young fibroblasts and known to be involved in cross-linking the ECM such as aggrecan, LOXL2, HAPLN1 lost during aging, creating an invasion-permissive microenvironment(Kaur et al., 2019).

1.9 UVA-induced Changes in Tumor Microenvironment (TME)

The development and progression of cancer are remarkably influenced by TME which is composed of noncancer stromal cells including immune cells, endothelial cells, and fibroblasts, and noncellular components such as chemokines, growth factors, cytokines, and ECM proteins(Liu et al., 2019). As the major player in tanning and photoaging, UVA irradiation initiates and activates a complex cascade of biochemical reactions in human skin. Similar to the effect of natural aging, UVA contributes to the generation of reactive oxygen species (ROS) that stimulates the inflammatory responses in the skin which lead to the depletion of cellular antioxidants and antioxidant enzymes (SOD, catalase), DNA damage, activation of the neuroendocrine system causing immunosuppression and increased synthesis and release of pro-inflammatory mediators from various skin cells(Pillai et al., 2005). Biochemically, ROS-mediated inflammation further activates the transcription of various matrix-degrading metalloproteases that regulate the proteolytic degradation of the skin ECM, leading to abnormal ECM and accumulation of non-functional matrix components which turnover cause increased degradation of collagen and elastic fibers in the dermis(Kawaguchi et al., 1996)(Pillai et al., 2005). Most skin cell

types such as fibroblasts, keratinocytes, and melanocytes synthesize MMPs which can be broadly classified into four major classes: collagenases which break down collagens (MMP-1 and MMP-8); gelatinases which degrade denatured collagens (MMP2 and MMP9); stromelysins, which have broad-spectrum specificity, and membrane-bound MMPs which are located mainly on tumor cells(Vincenti and Brinckerhoff, 2007). UVA has been shown to induce the expression of MMP1 in dermal fibroblasts in vivo and MMP1, MMP2, and MMP3 in cultured fibroblasts(Suganuma et al., 2010). Furthermore, the inflammation and ROS cause oxidative damage to cellular proteins, lipids, and carbohydrates, which accumulate in the epidermal and dermal compartments, contributing to the etiology of photoaging(Kang et al., 2001).

1.10 Comparison Between Natural Ageing and Photoaging

Given that ECM changes occur in both exposure to intrinsic aging and extrinsic UVA, we are interested in examining whether the effects of UVA on mediators of ECM homeostasis differ between young and aged human skin fibroblasts and whether that can create an environment that increases the malignant potential of melanoma.

To address this question, we will conduct a comparative gene expression analysis of young fibroblasts acutely exposed to doses of UVA. We hypothesize that acute exposure to UVA will induce changes in ECM-related gene expression in young fibroblasts that drive them towards an aged, tumor-promoting phenotype. We also expect that UVA-induced photoaged microenvironment will have a promoting effect on melanoma cells. We are proposing to test this hypothesis using the following methods.

2. MATERIALS AND METHODS

Cell Lines and Culture Conditions

2003-071-056 and 2003-071-032 young dermal fibroblast cell lines were obtained from the skin of a 28-year-old male healthy donor. AG13004, AG04157, GM13335 old dermal fibroblast cell lines were obtained from the skin of a 68-year-old male healthy donor. The fibroblasts were cultured in DMEM (Dulbecco-Vogt modification of Eagle's medium) (Invitrogen, Carlsbad, CA) supplemented with 10% fetal calf serum (Sigma-Aldrich), 100 U/mL penicillin, 100 µg/mL streptomycin (Sigma-Aldrich), and 4 mM L-Glutamine and cultured in 5% CO_2 at 37°C. Cells were fed with fresh medium every 3rd day and were passaged routinely at a confluence of ~80%. Cell stocks were fingerprinted using an AmpFLSTR Identifiler PCR Amplification Kit from Life Technologies at The Wistar Institute Genomics Facility.

Cell Viability – LIVE/DEAD Assay for Mammalian Cells

Fibroblasts were cultured inside 35 mm disposable Petri dishes for 2-3 days until acceptable cell density are obtained. Cells were washed gently with 500–1,000 volumes of Dulbecco's phosphate-buffered saline (D-PBS) to remove or dilute serum esterase activity generally present in the serum-supplemented growth medium. Cells were then treated with cytotoxic agents as required at any time before or concurrent with LIVE/DEAD reagent staining. The LIVE/DEAD® assay reagents were removed from the freezer and allow to warm to room temperature. An approximately 4 µM EthD-1 solution was made by adding 20 µL of the supplied 2 mM EthD-1 stock solution (Component B) to 10 mL of sterile, tissue culture–grade D-PBS, vortexing to

ensure thorough mixing an approximately 2 μM calcein AM was made by combining the reagents by transferring 5 μL of the supplied 4 mM calcein AM stock solution (Component A) to the 10 mL EthD-1 solution, vortexing the resulting solution to ensure thorough mixing. The resulting approximately 2 μM calcein AM and 4 μM EthD-1 working solution was then added directly to cells. The final concentration of DMSO was ≤ 0.1%, a level generally innocuous to most cells. 100–150 μL of the combined LIVE/DEAD® assay reagents with optimized concentrations were added to the surface of a 22 mm square coverslip so that all cells were covered with solution. Incubations were performed in a covered 35 mm disposable petri dish to prevent contamination or drying of the samples for 30-45 minutes at room temperature. Following incubation, about 10 μL of the fresh LIVE/DEAD reagent solution was added to a clean microscope slide. The wet coverslip was carefully (but quickly) inverted and mounted on the microscope slide using fine-tipped forceps, then was sealed to the glass slide. The labeled cells can be viewed under the fluorescence microscope.

Ultraviolet A Irradiation

Spectroline™ E-Series Handheld UV Lamp equipped with 312 nM UVA was used for UVA irradiation. Cells in passages 9 to 12 were seeded at 3.6×10^4 cells per 35mm plastic Petri dishes (in 2.5 mL) as the control groups and 4.5×10^4 cells per 35 plastic Petri dishes (in 2.5 mL) as the treated groups. Cells were grown for about 2-3 days to reach confluency. Thus, each Petri dish contains approx. 1.2×10^5 cells/cm^2 in the control groups and approx. 1.6×10^5 cells/cm^2 in the treated groups. On the treating day, two control group plastic Petri dishes and two treated group plastic Petri

dishes were washed three times with 1 mL of HBSS and transferred into a reduced volume of serum-free DMEM medium (2.5 mL). Then two treated group dishes were placed on a plastic shelf inside the machine and were irradiated from the top. The central area of the shelf allowed the homogeneous irradiation of two dishes. Actinometry gave an average light intensity of 1.65 mW/cm^2 ± 0.05 (8.91 J/cm^2). Cells were treated for 1.5 hours and then were transferred back into normal medium and culture conditions. The control groups were sham-irradiated, i.e. kept in the dark during the same time and under the same environmental conditions as the irradiated cells. Repeat treatment for three consecutive days. The protocol we designed for cell irradiation is shown in Figure 5.

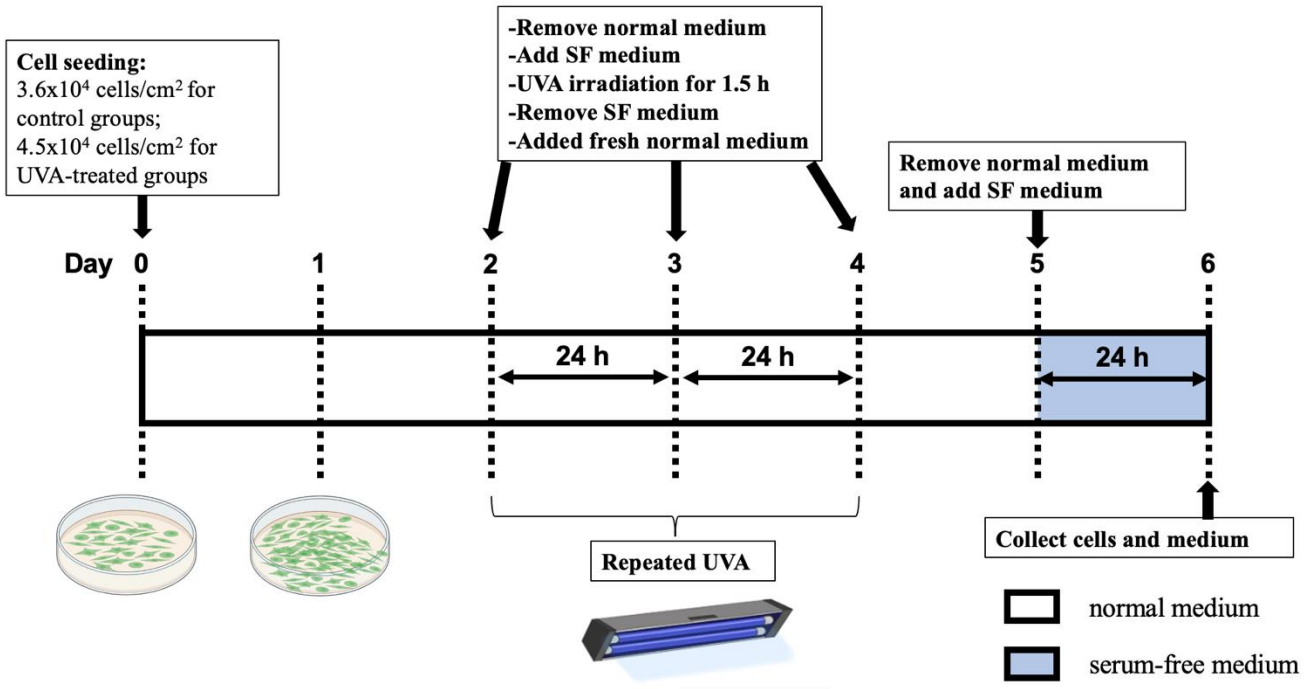

Figure 5. Representative diagram of cell irradiation protocol.

Medium Collection and Cell Harvest

After the third treatment of UVA irradiation, the cells were maintained in

DMEM medium and normal culture conditions for 24 hours, then washed them three times with 1 mL HBSS and replenished with 3 mL of serum-free DMEM. After 24 hours, remove 2.5 mL of the medium from each plate into a labeled 15 mL tube containing protease inhibitors: Phenylmethanesulfonyl fluomide solution (25 µL), 5 mg/ml Leupeptin Ready Made solution (25 µL) and 1 mM Pepstatin A (25 µL). Centrifuge the medium at 2000 rpm, 4°C for 10 mins, and then transfer the supernatant from the 15 mL tube to 3 mL syringe and filter the medium (~2 mL) through 0.22 µM syringe filter into a fresh 2 mL plastic microtube. Store the medium samples in -80°C.

After taking out the medium from the dishes, wash the dishes twice with 1 mL sterile PBS, then RIPA buffer was added to each plate (~50 µL/plate, dependent on the cell number). Cleaned scrapers were used to scrape each plate to collect cells and the lysate was transferred to 1.5 mL plastic microtubes. The lysate in the tubes was sheared by a 1 mL syringe with a 22G needle attached, and all tubes were placed on ice for 30 min. After lysates have finished processing, they were centrifuged at 13000 rpm, 4°C for 10 mins. After centrifugation, the supernatant was transferred to new 1.5 plastic microtubes stored at -80°C and the volume was measured and recorded.

Protein Quantification (BCA Assay)

The lysate of fibroblast cells was diluted 1:2 in ddH2O. 5 µL of each sample was added into duplicate microtubes. 10 µL of each standard reagent was also added into duplicate microtubes. Working solutions of BCA were prepared daily by mixing 50 parts of reagent A (BCA, sodium carbonate, sodium bicarbonate, bicinchoninic acid, and sodium tartrate in 0.1 M sodium hydroxide) with 1 part of reagent B ($CuSO_4$,

4%), as indicated by the manufacturer. 200 µL of BCA working solutions were pipetted into all microtubes. The microtubes were quickly placed in the reader and shaken for 30 s in a smooth motion before reading and they were kept for 30 mins at 37 °C. Then pipette 150 µL from all microtubes onto the wells of a 96-well plate. The absorbance at 562 nm of the microplate was read using a Villanueva reader.

Western Blotting and Development

Samples of lysate collected from the cell that had UVA-treated were mixed with sample buffer (8 µL), 10x reducing agent (3.2 µL), and a certain amount of RIPA buffer for a total of 32 µL. Samples were electrophoresed (130 V) on a 10% acrylamide resolving gel for 1 h when probing for β-catenin, MMP-1, and GAPDH. The gel was then soaked in 1× transfer buffer for 15 min [25× transfer buffer contains 300 mm Tris base (pH 8.3) and 2.4 m glycine). Protein transfer was done using iBlot Transfer Stacks by electroblotting onto polyvinylidene difluoride membrane for 7 min at 30 V. Blots were blocked in 10% nonfat dry milk solution for 1h. Then, the membrane was probed overnight with the antibody (1:1000 dilution) for β-catenin, the antibody (1:1000 dilution) for MMP-1, the antibody (1:1000 dilution) for GAPDH, in 5 ml of 10% milk solution made with wash buffer TBST. On the next day, the blots were washed with TBST in 10 min for three times. Then anti-rabbit immunoglobulin antibody (1:2000 dilution for β-catenin and MMP-1, 1:4000 for GAPDH) in 5 ml of 10% milk was added to the membrane and incubated for 1 h. After secondary antibody incubation, the blots were washed with TBST for 10 min for three times. The development was performed using Syngene G:Box Imager, antibody signals were

detected using enhanced chemiluminescence followed by autoradiography.

Instant Blue Protein Stain

The same preparation and methods of Western Blot were used on the fibroblasts culture medium. Electrophoresis was run at 130V for 1 hour. Gels were washed with distilled water and stained with Instant Blue (Expedeon) for 1 hour. Gels were imaged in Image Quant LAS 4000 under white light epi-illumination. Images were saved as a TIFF file with a size of 16-bit and a resolution of 1,392 x 1,040 pixels.

Lowry Protein Quantification Assay in Concentrated Medium

SF DMEM without phenol-red was collected from UVA-treated plates and control plates after a series of UVA treatments. Two tubes of medium were put into two Amicon Ultra-4 centrifugal filters (Merck Millipore Ltd. Tullagreen, Carrigtwohill) and centrifuged at 4°C, 4000 rpm for 1.5 hours to a 50 µL final volume. Prepare two microtubes and mix 15 µL of H2O/DMEM and 15 µL of 500 µg/mL Pierce Pre-Diluted BSA Standard #3 from ThermoFisher. 140 µL supplied 2x Folin-Ciocalteu Reagent was diluted in 140 µL H2O on the same day of use. Then 10 µL of each standard and unknown sample were pipetted into a 96-well plate in duplicate. 100 µL of modified Lowery reagent was added to each well at nearly the same moment using a multi-channel pipettor and immediately mixed on a plate mixer for 30 seconds. After mixing, the microplate was covered and incubated at room temperature for 10 minutes. Then 10 µL of prepared 1x Folin-Ci reagent was added

to each well using a multi-channel pipettor. The microplate was mixed immediately on a plate mixer for 30 seconds and covered for 30 minutes incubation at room temperature. After 30 minutes, the absorbance of each well was measured at 750 nm using a Villanueva reader. Finally, the concentration of experimental samples was calculated by using the pre-formatted protein calculation template.

Cell fixing and Immunofluorescence (IF) detection of γH2AX foci

2003-071-56 young fibroblasts were seeded onto 3 glass coverslips inside each plastic Petri dish, at 4.5×10^4 cells as the control group and 5.6×10^4 cells as the UVA dish, and incubated overnight. AG130004 aged fibroblasts were also seeded onto 3 glass coverslips at 4.5×10^4 cells/dish and incubated overnight. Same with the UVA irradiation protocol, the UVA group was irradiated with UVA for 3 consecutive days, the control group and the aged group were "mock" irradiated at the same amount of time. Interim two irradiations, one coverslip was taken out from each dish after 24 hours post-irradiation and put into a well of a 12-well plate. The coverslips were washed with 2 ml PBS twice and fixed with 4% PFA at room temperature for 20 minutes. Then the PFA was removed, coverslips were 2 ml PBS once again and kept in PBS at 4°C.

After collecting all coverslips from three groups, PBS in the well was removed and samples were incubated for 10 mins with PBS containing 0.25% Triton X-100 (permeabilization). Next, samples were incubated with PBS containing 2% BSA and 1% Triton X-100 for 40 min to block unspecific binding of antibodies. Then the

blocking buffer was removed, primary antibodies were diluted at the ratio of 1:400 in blocking buffer and incubated overnight at 4°C. Cells were washed in PBS and incubated with the appropriate secondary antibody (1:2000, Invitrogen) for 1 h at room temperature. Cells were then washed in PBS and mounted in Prolong Gold anti-fade reagent containing DAPI (Invitrogen). Images were captured on a Nikon eclipse Ti2 scanning laser confocal system.

Data and Statistical Analysis

Statistical data was collected using Image J software and was organized by Microsoft Excel. Reported data represents measurements carried out in triplicate or quadruplicate on three independent experiments. Repeated measures analysis of variance (ANOVA) was calculated between samples. For all experiments, Graphpad/Prism8 was used for plotting graphs and statistical analysis. All the data are presented as mean ± SD and subjected to statistical tests using the Student's t-test and the Peritz to compare two groups, respectively. A P-value less than 0.05 was considered significant. Significance was designated as follows: *, $p<0.05$; **, $p<0.01$; ***, $p<0.001$.

3. RESULTS

3.1 Morphological change of dermal fibroblasts induced by UVA irradiation

Fibroblasts in the dermis normally appear extensively flattened, which is critical for their role in the metabolism of ECM. They can change shape corresponding to the extracellular environment(Yamaba et al., 2016).

HDFs were cultured on plastic dishes in two groups (Control and UVA) and then irradiated with UVA light. The morphology of all fibroblasts was observed and assessed under 20x microscopy. Fibroblasts in the control group quickly attached to and uniformly spread on the dishes 2 days after seeding, gradually became more confluent and covered the entire inner surface (Figure. 5a). On day 6, after 24 hours staying in the SF medium, the increasing debris showed that some cells died after starvation, but most cells kept the normal flattened shape and the adhesion points between each other (Figure. 5a). In contrast, fibroblasts that have been irradiated with UVA for three consecutive days (Figure. 5b) were much less extensively spread than cells in the control group at Day 3. Most UVA-treated cells demonstrated a rounded/elongated shape and were not in intimate contact with surrounding cells. Besides, after the same process of starving in the SF medium, fibroblasts in the UVA group showed more damaged and collapsed appearance than cells in the control group. The whole irradiation process has been quintuplicated in both 2003-071-056 and 2003-071-032 cell lines, all the results of morphological changes and differences remain consistent across each round (data not shown). As fibroblasts in severely photoaged skin were observed to express a collapsed shape(Varani et al., 2004), our results showed the characteristic feature of photodamaged cells.

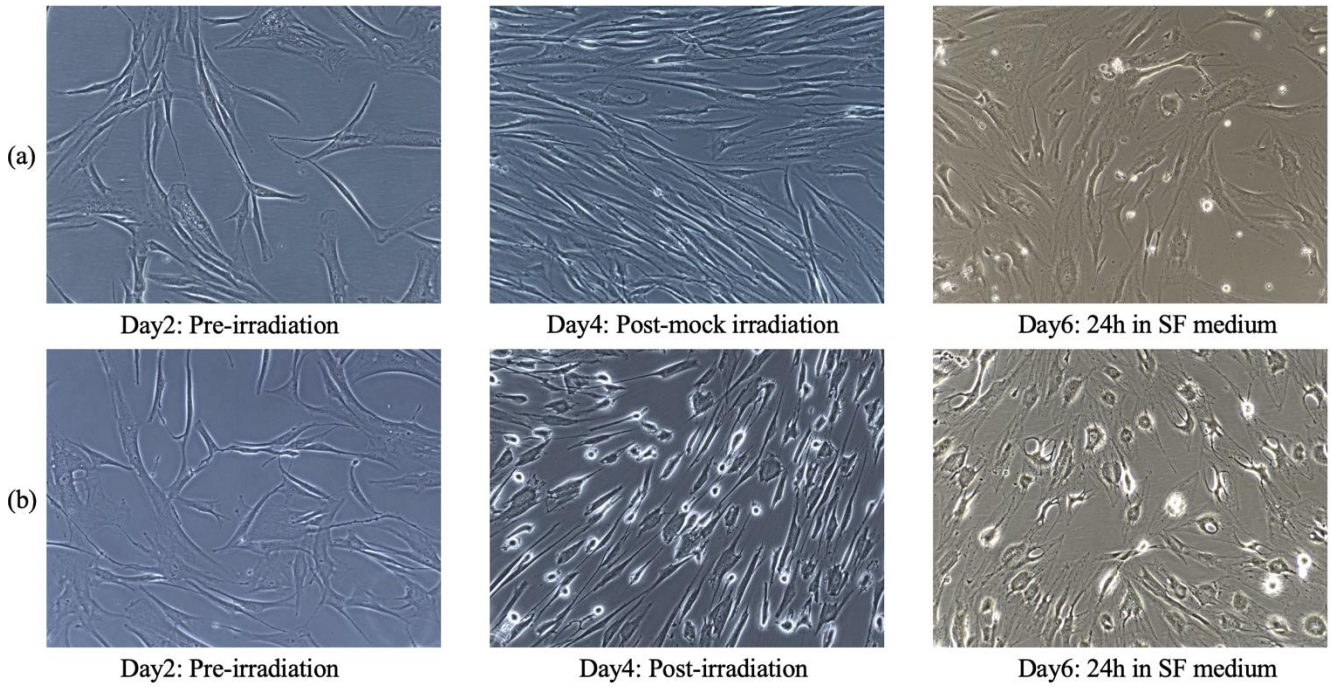

Figure 6. Illustration of (a) normal skin (b) photoaged skin

(a) Photographs of well-spread control group dermal fibroblasts at day1 before UVA treatment, day3 after the third irradiation, and day6 after 24 hours staying in serum-free medium. **(b)** Photographs of UVA group dermal fibroblasts at day1 before UVA treatment, day3 after the third irradiation, and day6 after 24 hours staying in serum-free medium. Cells were visualized under a microscope x20 magnification.

3.2 Changes in MMP-1 and β-catenin expression in HDFs induced by UVA irradiation

After showing the directly photodamaging morphology of fibroblasts induced by UVA, we investigated the accompanied changed cellular functions in fibroblasts by first assessing the intracellular expression level of photoaging-related signaling proteins in cell lysates. These experiments were performed three times independently in two young fibroblast cell lines, the complete result was shown in Appendix (Fig. S1). Since β-catenin is a key downstream effector of the canonical Wnt signaling pathway, which plays an important role in the motility, proliferation,

and differentiation of normal HDFs. Our western blotting results showed that β-catenin expression (Fig.6a), and the normalized level of β-catenin were significantly lower in UVA-irradiated cells than in the non-irradiated cells (Fig. 6b), this is consistent with the rounded cell shape and much fewer intercellular connections after irradiation. Previous studies have shown that UVA irradiation leads to photoaging through MMP-1 induction, and MMP-1 is also a proteolytic enzyme for degrading ECM proteins and causing a reduction in dermal collagen by fibroblasts(Bosch et al., 2015). Thus, MMP-1 expression was also analyzed by western blotting (Fig. 6a) and our results confirmed that the normalized expression of MMP-1 at the protein level was increased following UVA exposure (Fig. 6b). Collectively, these findings suggested that UVA irradiation could cause the dysfunction of fibroblasts and the disruption of ECM equilibrium by downregulating β-catenin expression as well as upregulating MMP-1 expression.

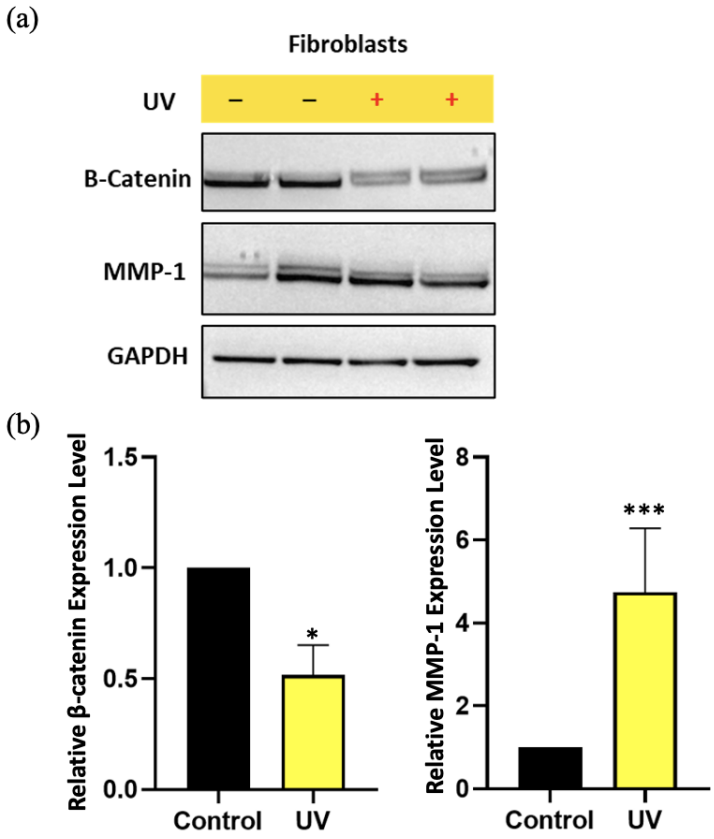

Figure 7. UVA irradiation-induced proteome changes in fibroblasts.

(a) β-catenin and MMP-1 expression in young fibroblast cell lines at protein level following three consecutive days of UVA irradiation, as determined by Western blotting, vs the expression in unirradiated young fibroblast as a negative control. Each group was duplicated. Western blot analyzes were normalized using GAPDH as a loading control. (b) Relative protein quantitative analysis of β-catenin and MMP-1 expression in irradiated vs unirradiated young fibroblasts as a control. In each group, the average β-catenin band intensity of two duplicates was normalized by the expression level of GAPDH, the average MMP-1 band intensity of two duplicates was normalized by the expression level of GAPDH and the total protein(μg) on the plate. Data are expressed as the mean ± SD, n = 2, *P < 0.05, **P < 0.01, ***P < 0.001.

3.3 Similar effects of natural aging and UVA irradiation on the expression of MMP-1 and β-catenin

Since natural aging is also associated with changed properties of skin cells

and ECM remodeling, we measured the expression of β-catenin and MMP -1 proteins in the lysate of four different aged fibroblast cell lines in order to compare the effects of aging with UVA-induced photoaging. In contrast to the two unexposed young fibroblast cell lines, downregulated β-catenin production and upregulated MMP-1 production were observed in aged fibroblasts shown by western blotting (Fig. 7a). which has less difference if not the same compared to the UVA irradiation data (Fig.7a, 7d). These data indicate that internal and UVA-induced external aging could have a similar influence on the function of fibroblasts and thus the remodeling of ECM.

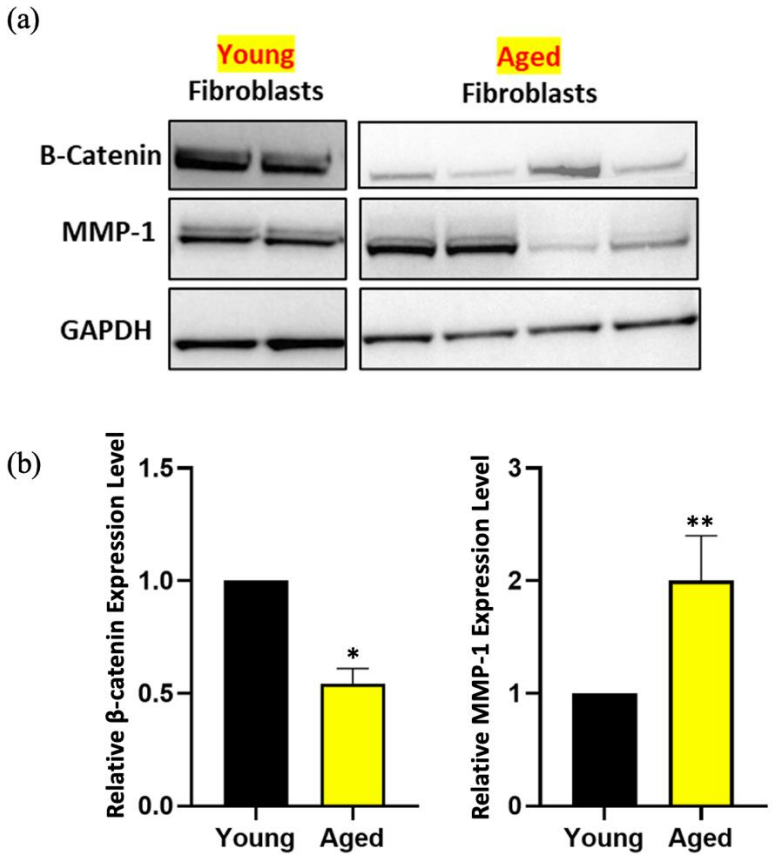

Figure 8. Proteome comparison between young and aged fibroblasts.

(a) Western blots images of β-catenin and MMP-1 expression in two unirradiated

young and four aged fibroblast cell lines respectively. (b) Relative protein quantitative analysis of β-catenin and MMP-1 expression in unirradiated young and aged fibroblast cell lines. In each group, the average β-catenin band intensity of two duplicates was normalized by the expression level of GAPDH, the average MMP-1 band intensity of two duplicates was normalized by the expression level of GAPDH and the total protein(μg) on the plate. Data are expressed as the mean ± SD, n = 2, 4, *P < 0.05 and **P < 0.01.

3.4 UVA irradiation increased the secretion of MMP-1 at the intercellular level

Since β-catenin and MMP-1 are both secreted proteins, we then measure the level of their presences in the medium to see if it is consistent with the changes in the cell lysate. The results of western blotting and densitometry showed that the expression level of MMP-1 in culture medium was elevated following UVA irradiation (Fig. 8a, 8b), which is in accordance with the findings in cell lysates. Taken together, our results confirmed that UVA exposure increases MMP-1 expression in HDFs, which might play a role in ECM remodeling during the process of photoaging.

We also conducted instant blue staining on another identical gel in the same experiment. Interestingly, opposite changes in two different proteins were observed when being compared in the exposed versus unexposed cells' medium (Fig.8c). We've sent the concentrated medium samples to the Proteomics and Metabolomics at Wistar Institute for complete characterization and quantification of proteomes and secretomes. Even though we cannot tell which band is what type of protein before we hear back from the proteomics analyzers, further investigations on UVA-induced secretome changes in HDFs are of importance for revealing the relationship between photoaging and TME.

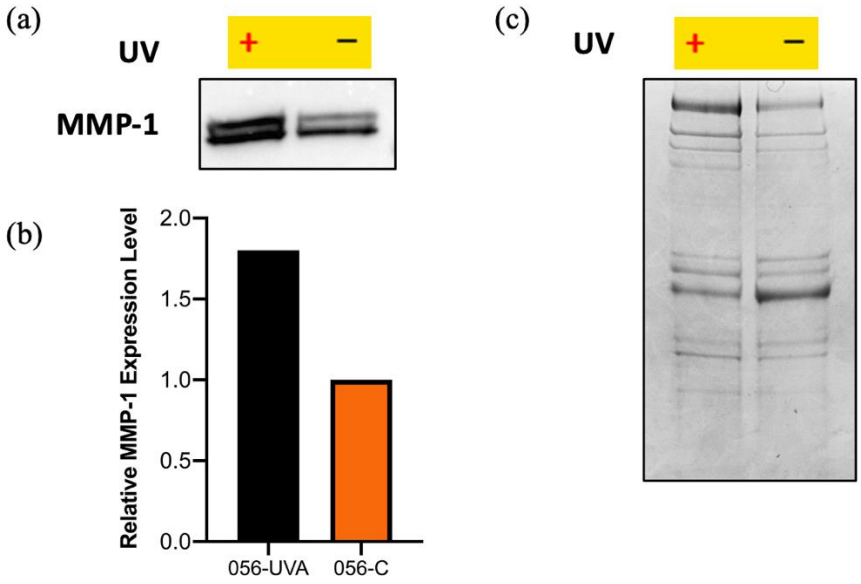

Figure 9. UVA-induced secretome changes in fibroblasts.

(a) Western blots image of MMP-1 expression in the medium of unirradiated and irradiated 2003-032-056 young fibroblast cells respectively. (b) Relative protein densitometry analysis of MMP-1 expression in the medium of unirradiated and irradiated 2003-032-056 fibroblast cells. In both groups, the average MMP-1 band intensity was normalized by the expression level of GAPDH and the total protein(μg) on the plate. (c) Instant blue staining image of complete secretomes in the medium of unirradiated and irradiated 2003-032-056 young fibroblast cells.

3.5 Increase in DNA damage induced by UVA irradiation

Since UVA irradiation can promote harmful effects including DNA damage, immunosuppression, and inflammation, as the direct or indirect consequences of increased production of ROS which destabilize biomolecules leading to mitochondrial damage, telomere shortening, and deterioration(Gasparrini et al., 2017). The accumulation of genetic alterations from defective repair of DNA damage is a universal cause of aging at a cellular level (Bautista-Niño et al., 2016). As the most critical DNA alternation, double-strand breaks (DSBs) are intensively investigated in live cells by immunocytochemical (ICC) staining in DNA repair protein foci(Kotenko

et al., 2013). For this reason, the constitutive level of the PI3-family phosphorylate core histone H2AX(γH2AX) as the DNA damage response kinase in response to the formation of DSBs, likely represents the presence of DSBs and DNA repair site(s)(Redon et al., 2011).

After observing the above similarities between photoaged and aged fibroblasts, we explored more on the effect of photoaging-related microenvironment at the molecular level and further compare it with the effect of internal aging. To do this, we measured the level of γH2AX foci in living fibroblasts by immunofluorescence staining after single UVA exposure. In the meantime, a set of control cells undergoing "mock treatment" and a set of aged cells were also measured for DNA damage. The observed level of *in vitro* indicator γH2AX is shown in Figure. 10, both the average and individual measurements of DNA damage in irradiated fibroblasts are significantly higher than the other two groups. Aged fibroblasts also presented more DNA damages than the unirradiated young fibroblasts. Collectively, both UVA-induced photoaging and natural aging are able to damage DNA in cultured dermal fibroblasts. But even low-dose of UVA exposure is more energetic than internal aging in damaging fibroblasts.

(a)

	UV	Control	Aged
Average GFP⁺ %	17.34%	6.61%	10.44%

(b)

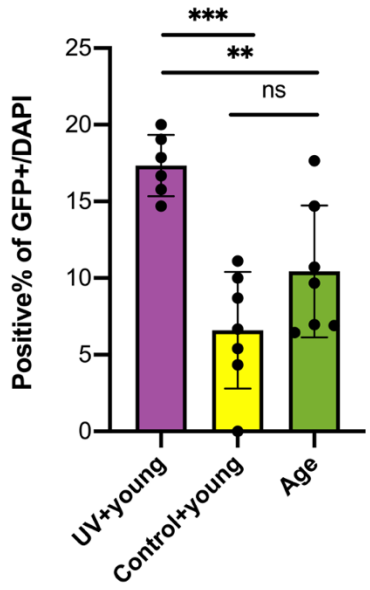

Figure 10. **Percentage of DNA damages in fibroblasts**

(a) Table of the average percentage of GFP⁺/DAPI representing the average percentage of DNA damages in the UVA-irradiated 2003-032-056 young HDFs, unirradiated young HDFs, and AG13004 aged HDFs respectively. (b) The plot of GFP⁺/DAPI percentages representing DNA damages in irradiated 2003-032-056 young HDFs, unirradiated young HDFs, and AG13004 aged HDFs respectively. Data are expressed as the mean ± SD, n = 6, *P < 0.05, **P < 0.01, ***P < 0.001.

4. DISCUSSION

Melanoma has been known as an exceptionally aggressive and therapy-resistant human cancer with an expanded incidence rate over years. The metastatic and recurrent melanoma with poor response rate and severe adverse events just makes the situation even worse, despite the prominent therapeutic progress in targeted therapies and immune checkpoint inhibitors(Zhou et al., 2015). In order to identify novel and more effective treatments, it's important to fully understand the driven factors underlying the pathology of melanoma formation and metastasis. It is widely acknowledged that over-exposure to UVR either natural or artificial is a complete carcinogen (El Ghissassi et al., 2009). As the main component of both natural and artificial UVR, UVA is detrimental as it penetrates deeply into the dermis and causes damage to the resident cells including fibroblasts(Holick, 2016). One ongoing question in the field is whether the continued exposure to UVA accelerates pro-tumorigenic phenotypes. Therefore, it is critically important to understand how young fibroblasts respond to UVA damage, and how that shapes their ability to drive tumor progression.

Here we showed UVA-induced morphological changes in young fibroblasts on plastic dishes from expanded to rounded, as a characteristic of photoaged cells. In the human dermis, fibroblasts are embedded in ECM and physically attached with the surrounding ECM(Yamaba et al., 2016). Therefore, the morphological change can be considered to be caused by the decreased amount of contact points and cell adhesion. It has been previously reported that instead of caused by decreased cell adhesion, the same change in the shape of fibroblasts under moderate dose of UVA irradiation was caused by the destruction of actin filaments which altered the cytoskeleton(Yamaba et al., 2016).

And the actin inhibitors inducing the morphological changes are also responsible for collagen reduction which leads to the wrinkle appearance as the hallmark of photoaged skin(Varani et al., 2004). To figure out the reason behind the shape change in this study, further staining tests are needed to verify the upstream main players.

In respect of cell adhesion and ECM metabolism, we hypothesized that UVA irradiation might alter the related gene expression in young HDFs. The results showed that β-catenin protein expression was reduced, while MMP-1 protein expression was upregulated in the exposed cells compared with the unexposed cells. Further, the level of MMP-1 was similarly increased in the media in which exposed fibroblasts were cultured. We also tried to plot β-catenin in the media, but its Western blotting intensity was too low to detect, thus we did not include that result here. As the key component in the canonical Wnt signaling pathway and cadherin-based cell adhesion, β-catenin can activate the downstream gene expression(Baarsma et al., 2011). The role of the Wnt/β-catenin signaling pathway in melanoma is complex and highly content-dependent, as documented evidence showed its dual role in both promotion and inhibition of melanoma(Gajos-Michniewicz and Czyz, 2016). Zhou's group observed blocked β-catenin inhibited the normal function of fibroblasts and promote melanoma development(Zhou et al., 2016). Consistent with their findings, the decreased β-catenin we observed indicated the dysfunction of normal HDFs, along with the increased MMP-1 which is responsible for denaturing ECM by cleaving collagen II. Further, a similar change of β-catenin and MMP-1 and increase of DNA damage were also shown across different lines of aged cells, implicating that UVA irradiation might induce changes in ECM-related gene expression in young fibroblasts that drive them towards an aged, tumor-promoting phenotype. Aging is an independent activator for the aggressive nature of melanoma by

promoting angiogenesis, ECM remodeling, metastasis, and so on(Kaur et al., 2016). Therefore, our study confirms the capability of UVA to induce the pre-mature photoaging in young fibroblasts and the consistency between photoaging and natural aging in disorganizing the normal function of HDFs as well as the normal structure of ECM (Fig. 11). Here we have only targeted β-catenin and MMP-1 as indicators for the relationship between fibroblasts and the surrounding microenvironment, it is worth targeting other factors alongside the canonical Wnt signaling pathway to reveal a more comprehensive picture of its role in melanoma.

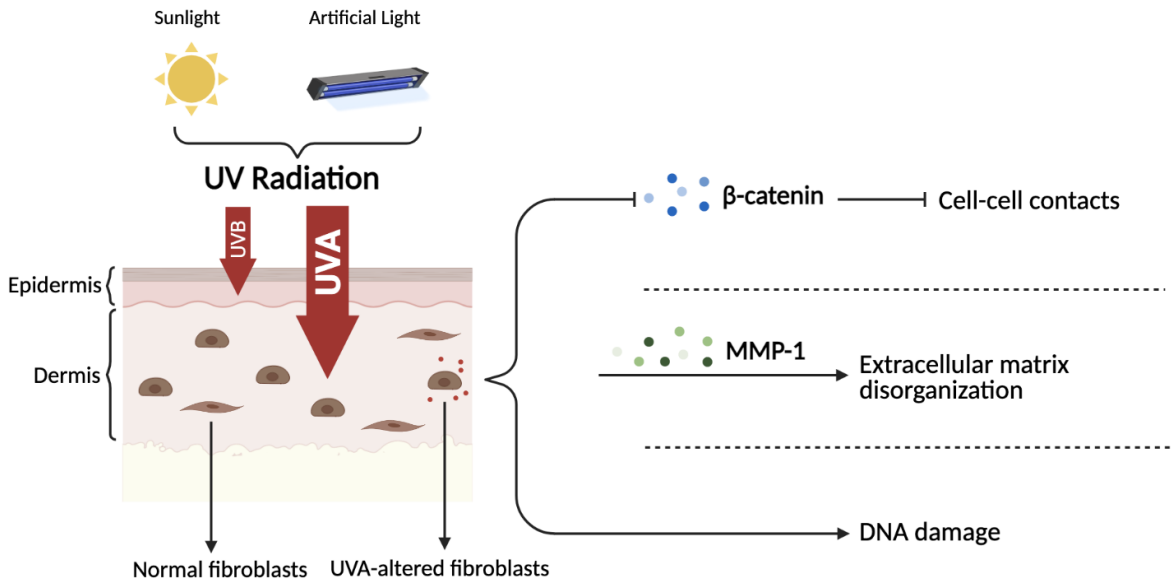

Figure 11. Summary scheme: Photoaging effects of UVA on dermal fibroblasts.

Overall, understanding the molecular mechanisms affected by UVA may reveal a more effective prevention method against melanoma and unique vulnerabilities in the melanoma microenvironment that can be targeted in order to overcome the disease.

However, this study is subjected to some limitations. First, among the triplicate

analyses on UVA-irradiated cell lysate, there is still a significant discrepancy. The possible factors affecting the result could be different cell lines (2003-071-56 cells generally performed better than 2003-071-032 cells), different cell passages, and operator error. Second, the results from the complete proteomics analysis are more dependable for elucidating the effects of photoaged fibroblasts on the ECM. But we have not received it at the time of the study's end. We accounted for uncertainty around such explanations by conducting sample concentrated medium analyses. Lastly, some unsolved questions might instruct the direction of future study. Can inhibiting UVA-induced morphological changes in HDFs be a possible way to suppress or reverse photoaging progression? Given the changed expression of ECM and adhesion proteins, does their RNA level changed in synchrony? How will aged fibroblasts react to continued UVA exposure and how does its reaction differentiate from the reaction of young counterparts? It is also required to use knockdown and overexpression methods to further analyze the impact of secretome changes on tumor cells' survival, proliferation, invasion, and resistance to drugs.

In conclusion, the finding in this study indicates that accumulated exposure to UVA can induce morphological changes of HDFs characterized in photoaged skin. More importantly, the following alteration in ECM and adhesion protein expression and DNA damage in young fibroblasts may drive them towards an aged, tumor-promoting phenotype which facilitated the migration of tumor cells. These analyses also help underscore the potential benefits of continued public health efforts to identify and implement strategies to prevent melanoma. Because the health risks increase as the prevalence of repeat sunburn and indoor tanning increases, further efforts to promote correct sun-protection and reduce indoor tanning might be effective in reducing the burden of melanoma in the United States and even worldwide.

5. Appendix

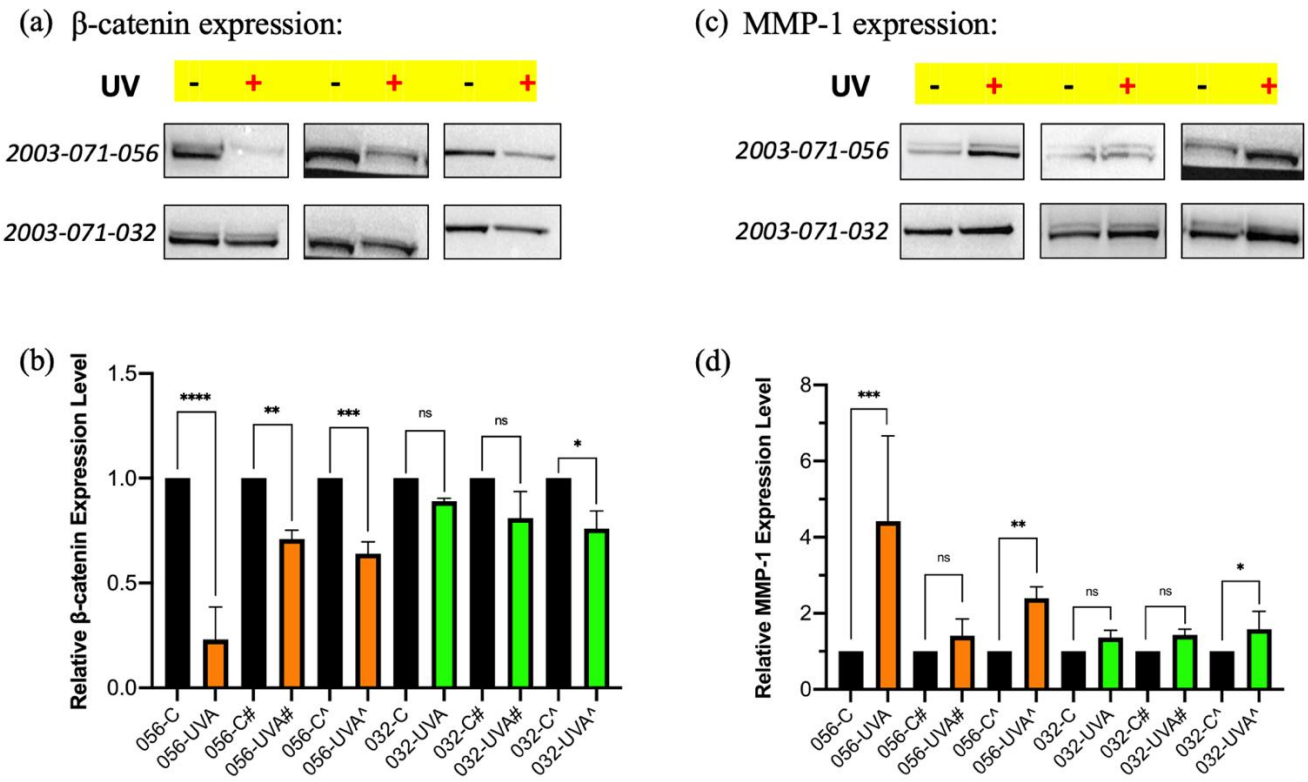

Figure S1. Triplicated UVA irradiation-induced proteomic changes in young fibroblasts

(a) β-catenin expression in 2003-071-056 and 2003-071-032 fibroblast cell lines after three consecutive days of UVA irradiation, as determined by Western blotting, vs the expression in unirradiated young fibroblast as a negative control. Here only one of the duplicates was shown. **(b)** Relative protein quantitative analysis of β-catenin expression in irradiated vs unirradiated fibroblasts as a control. In each group, the average β-catenin band intensity of two duplicates was normalized by the expression level of GAPDH. **(c)** MMP-1 expression in 2003-071-056 and 2003-071-032 fibroblast cell lines after three consecutive days of UVA irradiation, as determined by Western blotting, vs the expression in unirradiated young fibroblast as a negative control. Here only one of the duplicates was shown. **(d)** Relative protein quantitative analysis of MMP-1 expression in irradiated vs unirradiated fibroblasts as a control. In each group, the average MMP-1 band intensity of two duplicates was normalized by the expression level of GAPDH and the total protein(μg) on the plate. Data are expressed as the mean ± SD, n = 2, *P < 0.05, **P < 0.01, ***P < 0.001, ****P < 0.0001.

Bibliography

Agar, N.S., G.M. Halliday, R.S. Barnetson, H.N. Ananthaswamy, M. Wheeler, and A.M. Jones. 2004. The basal layer in human squamous tumors harbors more UVA than UVB fingerprint mutations: a role for UVA in human skin carcinogenesis. *Proc. Natl. Acad. Sci.* 101:4954–4959.

Akbani, R., K.C. Akdemir, B.A. Aksoy, M. Albert, A. Ally, S.B. Amin, H. Arachchi, A. Arora, J.T. Auman, and B. Ayala. 2015. Genomic classification of cutaneous melanoma. *Cell*. 161:1681–1696.

Anne, E. 2018. Melanoma–role of the environment and genetics. *Photochem. Photobiol. Sci.* 17:1853–1860.

Baarsma, H.A., A.I.R. Spanjer, G. Haitsma, L.H.J.M. Engelbertink, H. Meurs, M.R. Jonker, W. Timens, D.S. Postma, H.A.M. Kerstjens, and R. Gosens. 2011. Activation of WNT/β-catenin signaling in pulmonary fibroblasts by TGF-β 1 is increased in chronic obstructive pulmonary disease. *PLoS One*. 6:e25450.

Bai, H., M. Shu, M. Chen, A. Khan, and Z. Bai. 2018. Antioxidative and antiphotoaging activities of neferine upon UV-A irradiation in human dermal fibroblasts. *Biosci. Rep*. 38.

Balch, C.M., J.F. Thompson, J.E. Gershenwald, S. Soong, S. Ding, K.M. McMasters, D.G. Coit, A.M.M. Eggermont, P.A. Gimotty, and T.M. Johnson. 2014. Age as a predictor of sentinel node metastasis among patients with localized melanoma: an inverse correlation of melanoma mortality and incidence of sentinel node metastasis among young and old patients. *Ann. Surg. Oncol.* 21:1075–1081.

Bald, T., T. Quast, J. Landsberg, M. Rogava, N. Glodde, D. Lopez-Ramos, J. Kohlmeyer,

S. Riesenberg, D. Van Den Boorn-Konijnenberg, and C. Hömig-Hölzel. 2014. Ultraviolet-radiation-induced inflammation promotes angiotropism and metastasis in melanoma. *Nature*. 507:109–113.

Battie, C., S. Jitsukawa, F. Bernerd, S. Del Bino, C. Marionnet, and M. Verschoore. 2014. New insights in photoaging, UVA induced damage and skin types. *Exp. Dermatol.* 23:7–12.

Bautista-Niño, P.K., E. Portilla-Fernandez, D.E. Vaughan, A.H. Danser, and A.J.M. Roks. 2016. DNA damage: a main determinant of vascular aging. *Int. J. Mol. Sci.* 17:748.

Boivin, F.J., S. Sarin, J.C. Evans, and D. Bridgewater. 2015. The good and bad of β-catenin in kidney development and renal dysplasia. *Front. cell Dev. Biol.* 3:81.

Boniol, M., P. Autier, P. Boyle, and S. Gandini. 2012. Cutaneous melanoma attributable to sunbed use: systematic review and meta-analysis. *Bmj*. 345.

Bosch, R., N. Philips, J. Suárez-Pérez, A. Juarranz, A. Devmurari, J. Chalensouk-Khaosaat, and S. González. 2015. Mechanisms of Photoaging and Cutaneous Photocarcinogenesis, and Photoprotective Strategies with Phytochemicals. *Antioxidants*. 4:248–268. doi:10.3390/antiox4020248.

Castells, M., B. Thibault, J.-P. Delord, and B. Couderc. 2012. Implication of tumor microenvironment in chemoresistance: tumor-associated stromal cells protect tumor cells from cell death. *Int. J. Mol. Sci.* 13:9545–9571.

Cheon, S.S., P. Nadesan, R. Poon, and B.A. Alman. 2004. Growth factors regulate β-catenin-mediated TCF-dependent transcriptional activation in fibroblasts during the proliferative phase of wound healing. *Exp. Cell Res*. 293:267–274.

Chin, L. 2003. The genetics of malignant melanoma: lessons from mouse and man. *Nat.*

Rev. Cancer. 3:559–570.

Coelho, S.G., W. Choi, M. Brenner, Y. Miyamura, Y. Yamaguchi, R. Wolber, C. Smuda, J. Batzer, L. Kolbe, and S. Ito. 2009. Short-and long-term effects of UV radiation on the pigmentation of human skin. *In* Journal of Investigative Dermatology Symposium Proceedings. Elsevier. 32–35.

Cornil, I., D. Theodorescu, S. Man, M. Herlyn, J. Jambrosic, and R.S. Kerbel. 1991. Fibroblast cell interactions with human melanoma cells affect tumor cell growth as a function of tumor progression. *Proc. Natl. Acad. Sci.* 88:6028–6032.

Cuiffo, B.G., and A.E. Karnoub. 2012. Mesenchymal stem cells in tumor development: emerging roles and concepts. *Cell Adh. Migr.* 6:220–230.

D'Orazio, J., S. Jarrett, A. Amaro-Ortiz, and T. Scott. 2013. UV radiation and the skin. *Int. J. Mol. Sci.* 14:12222–12248.

Delmas, V., F. Beermann, S. Martinozzi, S. Carreira, J. Ackermann, M. Kumasaka, L. Denat, J. Goodall, F. Luciani, and A. Viros. 2007. β-Catenin induces immortalization of melanocytes by suppressing p16INK4a expression and cooperates with N-Ras in melanoma development. *Genes Dev.* 21:2923–2935.

Dhomen, N., and R. Marais. 2007. New insight into BRAF mutations in cancer. *Curr. Opin. Genet. Dev.* 17:31–39.

Dorsky, R.I., D.W. Raible, and R.T. Moon. 2000. Direct regulation of nacre, a zebrafish MITF homolog required for pigment cell formation, by the Wnt pathway. *Genes Dev.* 14:158–162.

Douki, T., A. von Koschembahr, and J. Cadet. 2017. Insight in DNA repair of UV-induced pyrimidine dimers by chromatographic methods. *Photochem. Photobiol.* 93:207–215.

Emri, G., G. Paragh, Á. Tósaki, E. Janka, S. Kollár, C. Hegedűs, E. Gellén, I. Horkay, G. Koncz, and É. Remenyik. 2018. Ultraviolet radiation-mediated development of cutaneous melanoma: An update. *J. Photochem. Photobiol. B Biol.* 185:169–175.

Erdmann, F., J. Lortet-Tieulent, J. Schüz, H. Zeeb, R. Greinert, E.W. Breitbart, and F. Bray. 2013. International trends in the incidence of malignant melanoma 1953–2008—are recent generations at higher or lower risk? *Int. J. cancer.* 132:385–400.

Fisher, G.J., Z. Wang, S.C. Datta, J. Varani, S. Kang, and J.J. Voorhees. 1997. Pathophysiology of premature skin aging induced by ultraviolet light. *N. Engl. J. Med.* 337:1419–1429.

Fuchs, E., and S. Raghavan. 2002. Getting under the skin of epidermal morphogenesis. *Nat. Rev. Genet.* 3:199–209.

Gaggioli, C., and E. Sahai. 2007. Melanoma invasion–current knowledge and future directions. *Pigment Cell Res.* 20:161–172.

Gajos-Michniewicz, A., and M. Czyz. 2016. Modulation of WNT/β-catenin pathway in melanoma by biologically active components derived from plants. *Fitoterapia.* 109:283–292.

Ganceviciene, R., A.I. Liakou, A. Theodoridis, E. Makrantonaki, and C.C. Zouboulis. 2012. Skin anti-aging strategies. *Dermatoendocrinol.* 4:308–319.

Gascard, P., and T.D. Tlsty. 2016. Carcinoma-associated fibroblasts: orchestrating the composition of malignancy. *Genes Dev.* 30:1002–1019.

Gasparrini, M., T.Y. Forbes-Hernandez, S. Afrin, P. Reboredo-Rodriguez, D. Cianciosi, B. Mezzetti, J.L. Quiles, S. Bompadre, M. Battino, and F. Giampieri. 2017. Strawberry-based cosmetic formulations protect human dermal fibroblasts against UVA-induced damage. *Nutrients.* 9:605.

El Ghissassi, F., R. Baan, K. Straif, Y. Grosse, B. Secretan, V. Bouvard, L. Benbrahim-Tallaa, N. Guha, C. Freeman, and L. Galichet. 2009. A review of human carcinogens—part D: radiation. *Lancet Oncol.* 10:751–752.

Guy, G.P., M. Watson, A.B. Seidenberg, A.M. Hartman, D.M. Holman, and F. Perna. 2017a. Trends in indoor tanning and its association with sunburn among US adults. *J. Am. Acad. Dermatol.* 76:1191–1193.

Guy, G.P., Y. Zhang, D.U. Ekwueme, S.H. Rim, and M. Watson. 2017b. The potential impact of reducing indoor tanning on melanoma prevention and treatment costs in the United States: An economic analysis. *J. Am. Acad. Dermatol.* 76:226–233. doi:10.1016/j.jaad.2016.09.029.

Hegde, U.P., N. Chakraborty, P. Kerr, and J.M. Grant-Kels. 2009. Melanoma in the elderly patient: relevance of the aging immune system. *Clin. Dermatol.* 27:537–544.

Hofmann, U.B., R. Houben, E.-B. Bröcker, and J.C. Becker. 2005. Role of matrix metalloproteinases in melanoma cell invasion. *Biochimie.* 87:307–314.

Holick, M.F. 2016. Biological effects of sunlight, ultraviolet radiation, visible light, infrared radiation and vitamin D for health. *Anticancer Res.* 36:1345–1356.

Holman, D.M., Z. Berkowitz, G.P. Guy Jr, A.M. Hartman, and F.M. Perna. 2014. The association between demographic and behavioral characteristics and sunburn among US adults—National Health Interview Survey, 2010. *Prev. Med. (Baltim).* 63:6–12.

Jimbow, K., and T.B. Fitzpatrick. 1975. Changes in distribution pattern of cytoplasmic filaments in human melanocytes during ultraviolet-mediated melanin pigmentation. The role of the 100-Angstrom filaments in the elongation of melanocytic dendrites and in the movement and transfer of melanosom. *J. Cell*

Biol. 65:481–488.

Kang, S., G.J. Fisher, and J.J. Voorhees. 2001. Photoaging: pathogenesis, prevention, and treatment. *Clin. Geriatr. Med.* 17:643–659.

Kaur, A., B.L. Ecker, S.M. Douglass, C.H. Kugel, M.R. Webster, F. V Almeida, R. Somasundaram, J. Hayden, E. Ban, and H. Ahmadzadeh. 2019. Remodeling of the collagen matrix in aging skin promotes melanoma metastasis and affects immune cell motility. *Cancer Discov.* 9:64–81.

Kaur, A., M.R. Webster, K. Marchbank, R. Behera, A. Ndoye, C.H. Kugel, V.M. Dang, J. Appleton, M.P. O'Connell, and P. Cheng. 2016. sFRP2 in the aged microenvironment drives melanoma metastasis and therapy resistance. *Nature.* 532:250–254.

Kawaguchi, Y., H. Tanaka, T. Okada, H. Konishi, M. Takahashi, M. Ito, and J. Asai. 1996. The effects of ultraviolet A and reactive oxygen species on the mRNA expression of 72-kDa type IV collagenase and its tissue inhibitor in cultured human dermal fibroblasts. *Arch. Dermatol. Res.* 288:39–44.

Kligman, L.H., and A.M. Kligman. 1986. The nature of photoaging: its prevention and repair. *Photodermatology.* 3:215–227.

Koch, S., S. Pettigrew, M. Strickland, T. Slevin, and C. Minto. 2017. Sunscreen increasingly overshadows alternative sun-protection strategies. *J. Cancer Educ.* 32:528–531.

Kotenko, K. V, A.Y. Bushmanov, I. V Ozerov, D. V Guryev, N.A. Anchishkina, N.M. Smetanina, E.Y. Arkhangelskaya, N.Y. Vorobyeva, and A.N. Osipov. 2013. Changes in the number of double-strand DNA breaks in Chinese hamster V79 cells exposed to γ-radiation with different dose rates. *Int. J. Mol. Sci.* 14:13719–13726.

Levental, K.R., H. Yu, L. Kass, J.N. Lakins, M. Egeblad, J.T. Erler, S.F.T. Fong, K. Csiszar, A. Giaccia, and W. Weninger. 2009. Matrix crosslinking forces tumor progression by enhancing integrin signaling. *Cell*. 139:891–906.

Liu, T., L. Zhou, K. Yang, K. Iwasawa, A.L. Kadekaro, T. Takebe, T. Andl, and Y. Zhang. 2019. The β-catenin/YAP signaling axis is a key regulator of melanoma-associated fibroblasts. *Signal Transduct. Target. Ther.* 4:1–15.

Lucas, R.M., S. Yazar, A.R. Young, M. Norval, F.R. De Gruijl, Y. Takizawa, L.E. Rhodes, C.A. Sinclair, and R.E. Neale. 2019. Human health in relation to exposure to solar ultraviolet radiation under changing stratospheric ozone and climate. *Photochem. Photobiol. Sci.* 18:641–680.

Mælandsmo, G.M., R. Holm, J.M. Nesland, Ø. Fodstad, and V.A. Flørenes. 2003. Reduced β-catenin expression in the cytoplasm of advanced-stage superficial spreading malignant melanoma. *Clin. Cancer Res.* 9:3383–3388.

Marino, G.E., and A.T. Weeraratna. 2020. A glitch in the matrix: Age-dependent changes in the extracellular matrix facilitate common sites of metastasis. *Aging and Cancer*. 1–11. doi:10.1002/aac2.12013.

Marzuka-Alcalá, A., M.J. Gabree, and H. Tsao. 2014. Melanoma susceptibility genes and risk assessment. *In* Molecular diagnostics for melanoma. Springer. 381–393.

Meyle, K.D., and P. Guldberg. 2009. Genetic risk factors for melanoma. *Hum. Genet.* 126:499–510.

Miller, J.R., and R.T. Moon. 1996. Signal transduction through beta-catenin and specification of cell fate during embryogenesis. *Genes Dev.* 10:2527–2539.

Min, W., X. Liu, Q. Qian, B. Lin, D. Wu, M. Wang, I. Ahmad, N. Yusuf, and D. Luo. 2014. The effects of baicalin against UVA-induced photoaging in skin fibroblasts. *Am. J.*

Chin. Med. 42:709–727.

Mouw, J.K., G. Ou, and V.M. Weaver. 2014. Extracellular matrix assembly: a multiscale deconstruction. *Nat. Rev. Mol. cell Biol.* 15:771–785.

Nakyai, W., A. Saraphanchotiwitthaya, C. Viennet, P. Humbert, and J. Viyoch. 2017. An in vitro model for fibroblast photoaging comparing single and repeated UVA irradiations. *Photochem. Photobiol.* 93:1462–1471.

Naylor, E.C., R.E.B. Watson, and M.J. Sherratt. 2011. Molecular aspects of skin ageing. *Maturitas*. 69:249–256.

Nilsen, L.T.N., T.N. Aalerud, M. Hannevik, and M.B. Veierød. 2011. UVB and UVA irradiances from indoor tanning devices. *Photochem. Photobiol. Sci.* 10:1129–1136.

O'Grady, A., C. Dunne, P. O'Kelly, G.M. Murphy, M. Leader, and E. Kay. 2007. Differential expression of matrix metalloproteinase (MMP)-2, MMP-9 and tissue inhibitor of metalloproteinase (TIMP)-1 and TIMP-2 in non-melanoma skin cancer: implications for tumour progression. *Histopathology*. 51:793–804.

Pérez-Sánchez, A., E. Barrajón-Catalán, M. Herranz-López, and V. Micol. 2018. Nutraceuticals for skin care: A comprehensive review of human clinical studies. *Nutrients*. doi:10.3390/nu10040403.

Pfeifer, G.P., and A. Besaratinia. 2012. UV wavelength-dependent DNA damage and human non-melanoma and melanoma skin cancer. *Photochem. Photobiol. Sci.* 11:90–97.

Pillai, S., C. Oresajo, and J. Hayward. 2005. Ultraviolet radiation and skin aging: roles of reactive oxygen species, inflammation and protease activation, and strategies for prevention of inflammation-induced matrix degradation–a review. *Int. J. Cosmet. Sci.* 27:17–34.

Postovit, L.-M., E.A. Seftor, R.E.B. Seftor, and M.J.C. Hendrix. 2006. Influence of the Microenvironment on Melanoma Cell Fate Determination and Phenotype. *Cancer Res.* 66:7833 LP – 7836. doi:10.1158/0008-5472.CAN-06-0731.

Quan, T., Z. Qin, W. Xia, Y. Shao, J.J. Voorhees, and G.J. Fisher. 2009. Matrix-degrading metalloproteinases in photoaging. *In* Journal of Investigative Dermatology Symposium Proceedings. Elsevier. 20–24.

Redon, C.E., A.J. Nakamura, O.A. Martin, P.R. Parekh, U.S. Weyemi, and W.M. Bonner. 2011. Recent developments in the use of γ-H2AX as a quantitative DNA double-strand break biomarker. *Aging (Albany NY)*. 3:168.

Ribero, S., D. Glass, and V. Bataille. 2016. Genetic epidemiology of melanoma. *Eur. J. Dermatology*. 26:335–339.

Schulz, I., H.-C. Mahler, S. Boiteux, and B. Epe. 2000. Oxidative DNA base damage induced by singlet oxygen and photosensitization: recognition by repair endonucleases and mutagenicity. *Mutat. Res. Repair*. 461:145–156.

Seftor, E.A., K.M. Brown, L. Chin, D.A. Kirschmann, W.W. Wheaton, A. Protopopov, B. Feng, Y. Balagurunathan, J.M. Trent, and B.J. Nickoloff. 2005. Epigenetic transdifferentiation of normal melanocytes by a metastatic melanoma microenvironment. *Cancer Res.* 65:10164–10169.

Shih, B.B., M.D. Farrar, M.S. Cooke, J. Osman, A.K. Langton, R. Kift, A.R. Webb, J.L. Berry, R.E.B. Watson, and A. Vail. 2018. Fractional sunburn threshold UVR doses generate equivalent vitamin D and DNA damage in skin types I–VI but with epidermal DNA damage gradient correlated to skin darkness. *J. Invest. Dermatol.* 138:2244–2252.

Siegel, R.L., K.D. Miller, and A. Jemal. 2016. Cancer statistics, 2016. *CA. Cancer J. Clin.*

66:7–30.

Slominski, A., D.J. Tobin, S. Shibahara, and J. Wortsman. 2004. Melanin pigmentation in mammalian skin and its hormonal regulation. *Physiol. Rev*. 84:1155–1228.

Slominski, A.T., M.A. Zmijewski, C. Skobowiat, B. Zbytek, R.M. Slominski, and J.D. Steketee. 2012. Sensing the environment: Regulation of local and global homeostasis by the skin neuroendocrine system. *Adv. Anat. Embryol. Cell Biol.* 212:v.

Smart Servier Medical Art. Available online: https://smart.servier.com/ (accessed on 29 September 2017).

Spathis, A., A.C. Katoulis, V. Damaskou, A.I. Liakou, C. Kottaridi, D. Leventakou, D. Sgouros, A. Mamantopoulos, D. Rigopoulos, and P. Karakitsos. 2019. BRAF mutation status in primary, recurrent, and metastatic malignant melanoma and its relation to histopathological parameters. *Dermatol. Pract. Concept*. 9:54.

Suganuma, K., H. Nakajima, M. Ohtsuki, and G. Imokawa. 2010. Astaxanthin attenuates the UVA-induced up-regulation of matrix-metalloproteinase-1 and skin fibroblast elastase in human dermal fibroblasts. *J. Dermatol. Sci.* 58:136–142.

Thakur, V., and B. Bedogni. 2016. The membrane tethered matrix metalloproteinase MT1-MMP at the forefront of melanoma cell invasion and metastasis. *Pharmacol. Res*. 111:17–22.

Trapani, G., V. Fanos, E. Bertino, G. Maiocco, O. Al Jamal, M. Fiore, Vi. Bembo, D. Careddu, L. Barberio, L. Zanino, and G. Verlato. 2020. Children with COVID-19 like symptoms in Italian Pediatric Surgeries: the dark side of the coin. *medRxiv*. 2020.07.27.20149757. doi:10.1101/2020.07.27.20149757.

U.S. Surveillance, Epidemiology, and End Results Program (SEER). SEER facts.

http://seer.cancer.gov/statfacts/html/melan.html. Accessed 24 Aug 2015

Varani, J., L. Schuger, M.K. Dame, C. Leonard, S.E.G. Fligiel, S. Kang, G.J. Fisher, and J.J. Voorhees. 2004. Reduced fibroblast interaction with intact collagen as a mechanism for depressed collagen synthesis in photodamaged skin. *J. Invest. Dermatol.* 122:1471–1479.

Varani, J., D. Spearman, P. Perone, S.E.G. Fligiel, S.C. Datta, Z.Q. Wang, Y. Shao, S. Kang, G.J. Fisher, and J.J. Voorhees. 2001. Inhibition of type I procollagen synthesis by damaged collagen in photoaged skin and by collagenase-degraded collagen in vitro. *Am. J. Pathol.* 158:931–942.

Vincensi, M.R., M. d'Ischia, A. Napolitano, E.M. Procaccini, G. Riccio, G. Monfrecola, P. Santoianni, and G. Prota. 1998. Phaeomelanin versus eumelanin as a chemical indicator of ultraviolet sensitivity in fair-skinned subjects at high risk for melanoma: a pilot study. *Melanoma Res.* 8:53–58.

Vincenti, M.P., and C.E. Brinckerhoff. 2007. Signal transduction and cell-type specific regulation of matrix metalloproteinase gene expression: Can MMPs be good for you? *J. Cell. Physiol.* 213:355–364.

Watson, M., E. Garnett, G.P. Guy, and D.M. Holman. 2014. The surgeon general's call to action to prevent skin cancer.

Watson, M., A.C. Geller, M.A. Tucker, G.P. Guy Jr, and M.A. Weinstock. 2016. Melanoma burden and recent trends among non-Hispanic whites aged 15–49 years, United States. *Prev. Med. (Baltim).* 91:294–298.

Weiss, S.A., J. Han, F. Darvishian, J. Tchack, S.W. Han, K. Malecek, M. Krogsgaard, I. Osman, and J. Zhong. 2016. Impact of aging on host immune response and survival in melanoma: an analysis of 3 patient cohorts. *J. Transl. Med.* 14:299.

Widlund, H.R., M.A. Horstmann, E.R. Price, J. Cui, S.L. Lessnick, M. Wu, X. He, and D.E. Fisher. 2002. β-Catenin–induced melanoma growth requires the downstream target Microphthalmia-associated transcription factor. *J. Cell Biol.* 158:1079–1087.

Yamaba, H., M. Haba, M. Kunita, T. Sakaida, H. Tanaka, Y. Yashiro, and S. Nakata. 2016. Morphological change of skin fibroblasts induced by UV Irradiation is involved in photoaging. *Exp. Dermatol.* 25:45–51.

Zaman, S., B.I. Chobrutskiy, J.S. Patel, B.M. Callahan, W.L. Tong, M.M. Mihyu, and G. Blanck. 2019. MMP7 sensitivity of mutant ECM proteins: an indicator of melanoma survival rates and T-cell infiltration. *Clin. Biochem.* 63:85–91.

Zhou, L., K. Yang, T. Andl, R.R. Wickett, and Y. Zhang. 2015. Perspective of targeting cancer-associated fibroblasts in melanoma. *J. Cancer.* 6:717.

Zhou, L., K. Yang, S. Dunaway, Z. Abdel-Malek, T. Andl, A.L. Kadekaro, and Y. Zhang. 2018. Suppression of MAPK signaling in BRAF-activated PTEN-deficient melanoma by blocking β-catenin signaling in cancer-associated fibroblasts. *Pigment Cell Melanoma Res.* 31:297–307.

Zhou, L., K. Yang, R. Randall Wickett, and Y. Zhang. 2016. Dermal fibroblasts induce cell cycle arrest and block epithelial–mesenchymal transition to inhibit the early stage melanoma development. *Cancer Med.* 5:1566–1579.

Resume

Weiqi Jiao

Apt 6C, 210 E. Redwood St, Baltimore, MD 21202 | (410)-522-8224 | annajwq@gmail.com

PROFILE

Detail-oriented research professional with 5-year experience executing and assisting with collaborative projects spanning the pharmaceutical, biotech, to public health sectors. Creative problem-solver, skilled in statistics, data development and programming, with passion for combining scientific background with strategical analysis and business skills to create value in ways that are financially and socially viable for better outcome in this Bio Era. Fluent in Mandarin and English.

EDUCATION

- **Master of Science** | Johns Hopkins Bloomberg School of Public Health — Sep. 2019 – May. 2021
  Major: Biochemistry and Molecular Biology — GPA: 4.0/4.0
- **Bachelor of Science** | China Pharmaceutical University — Sep. 2015 – Jun. 2019
  Major: Pharmaceutics — GPA: 88.1/100

CERTIFICATION

- **Data Science: Statistics and Machine Learning Specialization Credential** | Johns Hopkins University — Jul.2020
  Machine learning, Github, Data visualization, Statistics, Model selection
- **Data Science Specialization Credential** | Johns Hopkins University — Jul. 2020
  R programming, Github, Data manipulating and cleaning, Cluster analysis, Debugging
- **Applied Jewelry Professional Diploma** | Gemological Institute of America — Jun. 2020
  Jewelry Essentials, Colored Stone Essentials, Diamond Essentials

WORK / RESEARCH EXPERIENCE

Pharmacy Analyst | Initium Health — Jul.2020 – present

A public benefit corporation with innovative solutions for patients, administrators, and providers

- Assembled purchase resources for supply chain and inventory activities
- Placed bids on federal and state PPE solicitations, won several bids which generated $2000,000+ revenue.
- Engaged in two consulting cases to provide innovative solutions for Beth Israel Lahey Health (BILH) and Health Care Foundation of the Oranges (HCFO) on building out a profitable pharmacy business line including medication management, clinic-based specialty pharmacy and 340B programs.
- Worked with a health system to help them develop a systematic approach to conduct real-world evidence trial.
- Conducted primary and secondary research on clients' markets, customers and competitors.
- Familiar with U.S. healthcare system, pharmacy benefit management and organizations.

Research Assistant | Johns Hopkins Bloomberg School of Public Health — Feb.2020 – May.2021

- Designed a research strategy for personal project to investigate the effects of UVA irradiation on human dermal fibroblasts.
- Executed quantitative analysis on experimental data to explore biological mechanisms of photoaging.
- Interpreted, presented results at weekly meetings.
- Shared updated information, effectively communicated with lab members.

Lab Assistant | Johns Hopkins Bloomberg School of Public Health — Oct.2019 – Jan.2020

- Assisted post-doc fellows on several parallel projects, performed cell-level research on the mechanism of human Amyotrophic Lateral Sclerosis (ALS).
- Executed molecular genetic technologies to verify potential gene mutation and misfolded protein.
- Utilized Microsoft Office regularly to store data, model results, and generate reports.

Student Scholar | University of Southern California — Feb.2019 – May.2019

- Designed and performed an in-depth study on "The Inhibition Effect of Red Goji Berry (RGB) and Black Goji Berry (BGB) on Prostate Cancer and Glioma Cell Lines".

- Interpreted, presented results at weekly meetings.
- Troubleshot experiments and effectively collaborated with other members.

CONSULTING / LEADERSHIP

Pro Bono Consultant | Johns Hopkins Graduate Consulting Club Oct. 2020 – present
For Alera Partners cell therapy project: a global healthcare equity focused investment firm

- Reviewed and synthesized published clinical literature and unpublished resources
- Estimated the market potential of investigational candidate companies, their platforms and trials of various cell therapies.
- Analyzed data and develop economic model using Microsoft Excel to determine the probability of success of current trials
- Generated tables and graphs and prepared project deliverables including study reports and presentations
- Coordinated project activities to ensure timely completion of project

Member| Harvard Healthcare Club **|** Harvard University Aug.2020 – present

- Fostered the team for heading the Oncology international forum.
- Operated in the Design & Marketing Group.
- Designed and implemented sponsorship plans.
- Organized and maintained online social communities including social media and personal relationship management.
- Coordinated web operation and art design.

Leader of National College Student Innovation Project | China Pharmaceutical University
May.2017 – Jun.2018

- Lead and participated in this program funded by the Natural Science Foundation of Jiangsu Province.
- Communicated with members and instructor to decide our goal is to develop a novel drug delivery system which can target and deeply penetrate tumor tissue and intelligently release drugs.
- Positioned team members to use their skills optimally, Kept an eye on budgets and schedules.
- Organized weekly meetings, summarized, and reported progress to the department committee.

Leader of Snail Outdoor Hiking Club | China Pharmaceutical University Apr.2017 – Dec.2018
Organized the First Hiking Activity for Nanjing Public Welfare; Coordinated and organized between 100 members, rental firms and hotels; Lead seasonal hiking activities.

TECHNICAL SKILLS

- Microsoft Office Suite: profession
- Tableau: intermediate
- STATA: profession
- GraphPad Prism: profession
- Scientific writing: profession
- SQL: intermediate
- R programming: intermediate
- AutoCAD: intermediate

PUBLICATION

Self-assembled Block Polymer Aggregates in Selective Solution: Controllable Morphology Transition and Applications in drug delivery | Published by: Expert Opinion on Drug Delivery **|** May.2020
Authors: Weiqi Jiao[a,b], Hu Yang[c], Zimei Wu[d], Jianping Liu[a] and Wenli Zhang[a]